

IDENTIFYING POTENTIAL GEOTHERMAL RESOURCES FROM CO-PRODUCED
FLUIDS USING EXISTING DATA FROM DRILLING LOGS: WILLISTON BASIN,
NORTH DAKOTA

by

Anna M. Crowell
Bachelor of Science, Management/Computer Information Systems, Park University, 2003

A Thesis
Submitted to the Graduate Faculty

of the

University of North Dakota
in partial fulfillment of the requirements

for the degree of

Master of Science
Geology and Geological Engineering

Grand Forks, North Dakota
May
2011

This thesis, submitted by Anna M. Crowell in partial fulfillment of the requirements for the Degree of Master of Science from the University of North Dakota, has been read by the Faculty Advisory Committee under whom the work has been done and is hereby approved.

Chairperson

This thesis meets the standards for appearance, conforms to the style and format requirements of the Graduate School of the University of North Dakota, and is hereby approved.

Dean of the Graduate School

Date

PERMISSION

Title Identifying Potential Geothermal Resources from Co-Produced Fluids
 Using Existing Data from Drilling Logs: Williston Basin, North Dakota

Department Geology and Geological Engineering

Degree Master of Science

In presenting this thesis in partial fulfillment of the requirements for a graduate degree from the University of North Dakota, I agree that the library of this University shall make it freely available for inspection. I further agree that permission for extensive copying for scholarly purposes may be granted by the professor who supervised my thesis work or, in his absence, by the chairperson of the department or the dean of the Graduate School. It is understood that any copying or publication or other use of this thesis or part thereof for financial gain shall not be allowed without my written permission. It is also understood that due recognition shall be given to me and to the University of North Dakota in any scholarly use which may be made of any material in my thesis.

Signature _____

Date _____

TABLE OF CONTENTS

LIST OF TABLES	ix
ACKNOWLEDGEMENTS	x
ABSTRACT	xi
CHAPTER I	12
INTRODUCTION	12
Statement of Hypothesis	12
Geothermal Energy	12
The importance of geothermal energy	13
Heat Flow	15
Thermal Conductivity	18
Heat flow in the Williston Basin.....	20
Geothermal Energy in Sedimentary Basins	20
The Structure of the Williston Basin	21
CHAPTER II.....	23
METHODS	23
Temperature Correction and Reservoir Estimation	23
Prior work on the feasibility of using GIS for site selection.....	23
Bottom-Hole Temperature Corrections	23

Temperature Correction in the Williston Basin	25
Reservoir estimation within the Williston Basin	26
Creating the Geodatabase	28
Gathering the Data	28
Analyzing the Data	29
CHAPTER III	30
RESULTS	30
Overview.....	30
The Formations	30
Pennsylvanian: Tyler formation.....	30
Mississippian: Heath, Otter, Kibbey, Charles, Mission Canyon, and Lodgepole formations	31
Devonian: Bakken, Three Forks, Birdbear, Duperow, Souris River, Dawson Bay, Prairie Evaporite, Winnipegosis and Ashern formations ...	32
Silurian: Interlake formation.....	32
Ordovician: Stonewall, Stony Mountain, Red River, and Winnipeg formations	33
Cambrian: Deadwood formation.....	33
CHAPTER IV	35
CONCLUSION.....	35

Results of the bottom-hole corrections	35
Results of the Reservoir Estimate	35
Potential locations for commercial power plants.....	35
Areas of high water flow.....	35
Summary	36
APPENDICES	38
APPENDIX A.....	39
Figures.....	39
APPENDIX B	76
Tables.....	76
APPENDIX C	80
List of Acronyms	80
SOURCES CITED.....	82

LIST OF FIGURES

Figure 1 -- The Geothermal Map of United States (Reprinted with Permission, Blackwell and Richards, 2004)	40
Figure 2 -- Inset of the Geothermal Map of the United States showing Williston Basin detail (Modified from Blackwell and Richards, 2004).....	41
Figure 3 -- The Williston Basin, showing the Nesson and Cedar Creek Anticlines. (Modified from Heck et.al., 2000)	42
Figure 4 -- Graph of the Harrison Equation (Equation from Blackwell and Richards, 2004)	43
Figure 5 -- Temperature/Depth (TD) Plot from Blackwell and Richards, 2004a. (Reprinted with Permission)	44
Figure 6 - Graph of Uncorrected BHT Values.....	45
Figure 7 -- Graph of BHT Values after the Harrison Correction	46
Figure 8 -- Graph of BHT values after SMU Correction. The blank areas are a result of the correction method and may be caused by an inaccurate estimate of the local geothermal gradient.....	47
Figure 9 -- Plot of All Wells in North Dakota, as of June 2010.....	48
Figure 10 -- Plot of all wells in North Dakota with BHT data	49
Figure 11 -- Plot of all wells in North Dakota with formation thickness data.....	50
Figure 12 -- Example of BHT Interpolation	51
Figure 13 -- Example of polygon used to determine area	52
Figure 14 -- Estimate of the reservoir area in the Tyler formation.....	53
Figure 15 -- Isopach map of the Pennsylvanian Tyler formation.....	54
Figure 16 -- Formation surface map of the Pennsylvanian Tyler formation.....	55
Figure 17 -- Estimate of the reservoir area in the Mississippian formations.....	56

Figure 18 -- Isopach map of the Mississippian formations	57
Figure 19 -- Formation surface map of the Mississippian formations.....	58
Figure 20 -- Estimate of the reservoir area of the Bakken formation.....	59
Figure 21 -- Estimated reservoir area of the Three Forks formation.....	60
Figure 22 -- Estimate of the reservoir area for the other Devonian formations	61
Figure 23 -- Isopach Map of Other Formations in the Devonian Period.....	62
Figure 24 -- Formation surface map of the Devonian formations.....	63
Figure 25 -- Estimate of the reservoir area for the Silurian Interlake formation.....	64
Figure 26 -- Isopach map of the Silurian Interlake formation.....	65
Figure 27 -- Formation surface map of the Silurian Interlake formation	66
Figure 28 -- Estimate of the reservoir area for the other Ordovician formations	67
Figure 29 -- Estimate of the reservoir area for the Winnipeg formations.....	68
Figure 30 -- Isopach Map for the Ordovician formations	69
Figure 31 -- Formation surface map for the Ordovician formations	70
Figure 32 -- Estimate of the reservoir area for the Deadwood formation	71
Figure 33 -- Isopach map of the Cambrian Deadwood formation.....	72
Figure 34 -- Formation surface map of the Cambrian Deadwood formation.....	73
Figure 35 -- Raster image of the January 1985 BBL data interpolated	74
Figure 36 -- Abandoned and Dry Wells in High Flow Rate Areas.....	75

LIST OF TABLES

Table	Page
1. The estimated recoverable power based on the range of binary power plant efficiencies	50

ACKNOWLEDGEMENTS

The author wishes to thank Dr. William Gosnold, Dr. Lance Yarbrough, Dr. Michael Gaffey, Dr. Richard Lefever, Julie Lefever, Dr. Lorraine Manz, James “Josh” Crowell, James Crowell II, Vicky Morrisette and Jessie Hagemeister.

ABSTRACT

With the current need for technology that will allow for environmentally-friendly power generation, geothermal power has become an attractive resource given its low environmental impact and potential cost savings. One specific resource is co-produced water from oil wells that are not currently producing, but can yield formation waters that are both high enough in temperature and fluid volume to operate the turbines of binary geothermal power systems. The data required to identify sites, i.e. bottom-hole temperatures (BHT), latitude, longitude, total depth of hole (TD) in meters, the identification number, and the amount of water produced in gallons, can be mined from well logs that exist in various data systems.

Utilizing this data together with a Geographical Information System (GIS) software package, one can optimize the search for an ideal location for a binary power plant. I am analyzing data from the North Dakota Industrial Commission database for the North Dakota portion of the Williston Basin, with which I have created a report on potentially economically productive power plant locations along with a fully interactive map of western North Dakota.

CHAPTER I

INTRODUCTION

Statement of Hypothesis

Geothermal energy in oil and gas settings has the potential to offset fossil fuel energy use. Temperatures sufficient for geothermal power production occur in most oil and gas producing sedimentary basins. Identification of optimal locations for geothermal development using co-produced fluids from oil and gas wells can be inexpensively accomplished using existing well log data.

Geothermal Energy

A geothermal gradient map of North America based on bottom-hole temperature data acquired during well logging operations provided information useful for determining subsurface temperatures (Kehle, et al., 1970). However, bottom-hole temperature accuracy was found to be an issue and it continues to be a significant problem today (Blackwell and Richards, 2004; Harrison et al., 1983). Two methods of correction will be examined and best results will be quantified.

The key factors that determine the overall power production recoverability of geothermal resources in the Williston Basin are: producible fluid volume, fluid production rate, fluid temperature, and the economics of power plant installation. Producible fluid volume is determined by the size of the reservoir, porosity of the reservoir rock, and the estimated recovery rate (Sorey, 1982). Fluid production rate is determined by the porosity and permeability of the formation, and determines the rate at which the well can be pumped. Fluid

temperature determines how much thermal energy can be mined from a formation (i.e., the higher the temperature, the more energy can be recovered). The economics of installation are determined by two parameters; accessibility and sufficient fluid production (Tester et al, 2006).

Sorey et al. (1982) analyzed low temperature geothermal resources in sedimentary basins for the purpose of determining how much thermal energy a reservoir can yield over a 30-year period. A model was created in which evenly spread wells accessed geothermal fluids at 31.5 L/s (Liters per second) with a maximum drawdown of 152m (meters), after which the recoverable energy was estimated for each type or size of sedimentary basin. For a large sedimentary basin, Sorey (1982) determined that a thermal energy recovery rate of 0.1% was possible for power production over a 30 year period.

To accomplish the analysis of energy in the Williston Basin, the following parameters were defined; what BHT is sufficient, how many wells must be used to provide an appropriate flow rate for a geothermal power plant, and what is the recoverable energy of the resource. The production capacity of geothermal energy, the importance of heat flow, the need for thermal conductivity measurements, and the economic feasibility of utilizing co-produced fluids will be discussed.

The importance of geothermal energy

Heat flow at the surface of the continental crust averages 59 mW/m^2 (milliwatts per meter squared) (Tester et al., 2006). This energy currently escapes into space and is wasted, but could be harnessed for a variety of uses, including

power production. Producing electrical power from hot water contained in sedimentary basins is an innovative concept.

“Collecting and passing the (co-produced) fluid through a binary electrical power plant would take some engineering, but is a relatively straightforward process since most of the produced fluid is already passed to a central collection facility for hydrocarbon separation and water disposal (McKenna and Blackwell, 2005).”

“Piggy-backing on existing infrastructure should eliminate most of the need for expensive drilling and hydrofracturing operations, thereby reducing the majority of the upfront cost of geothermal electrical power production (McKenna and Blackwell, 2005).” Approximately \$4 per barrel of oil revenue was needed to offset oil field electrical costs in 2005 (McKenna and Blackwell).

Eighty-five percent of the energy used in the United States is produced from fossil fuels (Herzog and Golomb, 2004). Geothermal energy has little to no greenhouse gas emissions, but a 1,000 MW (Megawatt) pulverized coal-fired power plant emits between six and eight Mt/yr (Megaton per year) of CO₂ (Herzog and Golomb, 2004). Geothermal energy has thus emerged as an important resource.

Geothermal energy is also neither a new idea nor unique to the United States. Studies have been funded by the Department of Energy since the mid-1970s, producing such works as Circular 726, 790, and 892 (USGS), which examined the resource base for hydrothermal energy in the United States and developed some methods for evaluating the resource. The Former Soviet Union built the first true binary power plant at Paratunka in 1967 on the Kamchata peninsula. The power plant used 81° C water and produced 680 kWe (killiwatts electric) (Lund et al., 2008).

Exploitation of geothermal energy makes sense for more reasons than just the harnessing of otherwise wasted energy and climate conservation, especially when considering co-produced fluids. Co-produced water comprises approximately 98% of the total volume of exploration and production waste (Veil et al., 2004). In the United States, oil companies average seven barrels of water to one of oil; however, the ratio in the Williston Basin is quite a bit lower, starting at approximately 3 to 1 with the ratio increasing over the lifetime of the well (Veil et al., 2004).

The quantity of geothermal energy found in the Inyan Kara (Cretaceous), Mission Canyon (Mississippian), Duperow (Devonian), and Red River formations (Ordovician) in the Williston Basin may exceed the energy present in oil since, with a recovery factor of just 0.1 percent, the accessible resource base was found to be $13,500 \times 10^{18}$ J (Joules) (Gosnold, 1984).

Heat Flow

Heat Flow is the driving force behind geothermal energy, and the reason that continuous power production can be achieved. It is important, therefore, to understand the mechanism of heat flow as well as the evolution of heat flow studies, particularly as they apply to the United States. The temperature of the earth increases with depth at a rate of approximately 30°C (Celsius) per kilometer (Lund et al., 2008). "Terrestrial heat flow is defined as the quantity of heat escaping per unit time from the Earth's interior across each unit area of the Earth's solid surface (Pollack, 1982)." Heat escaping from the Earth comes from two main sources; convection and conduction from the mantle (approximately 60%)

and from the radioactive elements ^{232}Th , ^{235}U and ^{238}U , and ^{40}K (40% all together) (Pollack, 1982). Heat flow can be represented by Fourier's law, since the heat travels mostly by conduction, and can be determined by the equation $Q = -\Lambda \Gamma$, where Q is the heat flux factor, $-\Lambda$ is the thermal conductivity, and Γ is the local temperature gradient.

How heat flow measurements are taken, why the data must be corrected, and how those corrections are made are also important to understand. Borehole data is obtained by sending a probe down a well and logging the resistivities at intervals as the probe descends, after which the resistivities are converted to degrees Celsius. Some parameters for the measurements are necessary; such as only using wells deeper than 200 meters which were at equilibrium, from well mapped and well understood areas (Roy et al., 1968). The data also needs to be corrected for topography, structure, thermal conductivity and water movement (Roy et al., 1968; Roy, Blackwell, and Decker, 1972).

Regional heat flow is affected by many phenomena; such as localized radioactivity, crustal thickness and water advection (Lachenbruch, 1970). There is an exponential decrease of heat production with depth of the crust in plutonic rocks (Lachenbruch, 1970). There is also a linear relationship between heat flow and heat production in plutonic rocks, since the "local variability of heat flow in crystalline terrain is due primarily to lateral variations in upper crustal heat production (Blackwell, 1971)." As the lithosphere ages, it gets thicker and creates a thermal boundary layer, while a thinner crust always yields a higher heat flow (Crough, 1976). A general heat flow map which recognized the importance of

tectonic settings and regional differences was created by Lachenbruch and Sass in 1977, after the nature of heat flow; radioactivity and advection of groundwater were examined.

Geologic history of an area also affects heat flow. The surface heat flow on continents is controlled by the last orogenic event, distribution of heat-producing elements, and erosion (Selater et al., 1980). While heat flow is typically higher with recent tectonic activity, the relationship between crustal age and heat flow is not simple (Morgan, 1984). "The main factors controlling temperatures within the lithosphere and surface heat flow are the quantity and distribution of heat producing elements within the lithosphere (Morgan, 1984)." The lithosphere is divided into three zones; the upper near surface zone (which is directly affected by surface processes), the middle interval zone (which responds to heat balancing) and the lower boundary interaction between the lithosphere and asthenosphere (Morgan, 1984). The variables involved in computing continental heat flow make it too complex to use a simple equation, unlike oceanic heat flow (Morgan, 1984). Thermal regimes are directly related to variations in lithospheric thickness (Morgan and Gosnold, 1989).

Observed fluctuations in heat flow across a small area are often dramatic. Boreholes at equilibrium were logged to investigate how a complex geological structure might influence terrestrial heat flow, with the results that a system of groundwater flow could cause observed variation (Lewis and Becke, 1977). 55,244 BHTs from 28,260 wells in the Williston Basin were studied with the result that the basins heat flow patterns were influenced by water movement

(Majorowicz, 1984). Heat advection due to water movement can significantly alter the thermal profile of a basin (Gosnold, 1991). "High density brines divert freshwater flow around the central part of the Williston Basin (Gosnold, 1991)."

The question of whether or not heat flow can be used alone as a basis for assessing the magnitude of a geothermal resource was addressed in 2005 by Williams. Near-surface heat flow measurements provide a direct measurement of the natural heat flux required to maintain the hydrothermal system, and thus yield an approximate estimate of the potential renewable level of production (Williams, 2005). Deep reservoirs require less additional heat to maintain high temperatures, and heat flow is an important tool for characterizing shallow or large geothermal resources (Williams, 2005).

A method for creating a useable database for heat flow and other geothermal data was determined necessary in 1981 (Steele et al.). The data must be collected, what corrections needed to be made and what parameters needed to be set, were determined and then incorporated into a flow chart (Steele et al., 1981). The task was then to "show as accurately and completely as possible the state of knowledge of the geothermal field of the continent in all its variations (Blackwell and Steele, 1991)," which eventually lead to Figure 1, the Geothermal map of North America (Blackwell and Richards, 2004).

Thermal Conductivity

There are two measurements generally used for getting the data needed to determine heat flow: thermal conductivity, and bottom-hole temperature measurements, of which thermal conductivities are more precise and do not

require the corrections that bottom-hole measurements need. Thermal conductivity measurements can be used to estimate surface heat flow (Simmons, 1961). In situ thermal conductivity measurements are the most desirable for heat flow determinations (Simmons, 1961).

The divided bar setup for measuring thermal conductivities of rock, still recognizable in laboratories today, was developed by Birch (1950). The apparatus measured cylindrical pieces of rock, with parallel sides that were placed in a pressuring device which also has a substance of known thermal conductivity in line with the sample. A dynamically controlled heat source regulated heat on one side of the sample with a dynamically controlled heat sink on the other side. The system was allowed to reach thermal equilibrium, after which temperature measurements were taken by thermal couples. The thermal couples were placed to measure temperature across a substance with a known thermal conductivity and across the unknown sample, and the results were used to calculate the thermal conductivity of the unknown sample.

A method for obtaining thermal conductivity measurements without using a whole rock sample was developed by Sass et al. (1971). Rock chips with a known mass were inserted into a container filled with water, after which results were obtained that were estimated to be accurate within a 10% margin of error. The 10% margin of error was deemed acceptable since it is approximately the same as the variations in conductivity that are found in situ due to heterogeneity (Sass et al., 1971).

Heat flow in the Williston Basin

The AAPG dataset (Kehle, et al., 1970) was examined using a new methodology created by Blackwell et al. (1991), and resulted in The Geothermal Map of North America (Figure 1), published by Blackwell and Richards in 2004. This map shows that the Williston Basin stands out as an area of relatively high heat flow (Figure 2). 8,400 BHT's from the Canadian part of the Williston Basin were analyzed and evidence found to support the idea that hydrodynamics may affect the regional heat flow (Majorowicz et al., 1986). To account for hydrological variations, the usual heat flow equation was not used; instead, a temperature gradient based on a least squares equation was created (Majorowicz et al., 1986). Comparing these heat flow values for different formations, a positive correlation was discovered between the scale of the hydraulic head and higher heat flow for that portion of the Williston Basin (Majorowicz et.al., 1986). High heat flow values in the mid-continent region could be partially due to advection in the Williston Basin as the denser saline water diverts freshwater flow into the upper formations (Gosnold, 1990).

Geothermal Energy in Sedimentary Basins

“Using co-produced hot water, available in large quantities at temperatures up to 100°C or more from existing oil and gas operations, it is possible to generate up to 11,000 MWe (Megawatts electric) of new generating capacity with standard binary-cycle technology, and increase hydrocarbon production by partially offsetting parasitic losses consumed during production (Tester et al., 2006).” Mobilizing a rig to deepen a well can cost between \$700,000 and \$1,000,000, but drilling a new well can cost approximately

\$1,800/meter (Tester et al., 2006). In comparison, utilizing an existing well may not require any modification at all, depending on the depth of the reservoir and the temperature necessary for power production. The existing oil wells also already have road and electrical infrastructure in place, further reducing the set up costs for geothermal power plants. The low cost of utilizing existing oil wells for geothermal power production satisfies the first requirement identified by Tester et al.(2006); that of accessibility. The lower flow rate found in sedimentary basins are of concern (McKenna and Blackwell, 2005), but can be overcome by using more than one well to feed a single geothermal plant, satisfying the second requirement set forth by Tester et al. (2006); that of sufficient productivity.

The Structure of the Williston Basin

The Williston Basin is an intracratonic basin of approximately 133,644 square kilometers with at least two major structures: The Nesson and Cedar Creek anticlines (Figure 3) (Carlson and Anderson , 1965). The basin contains, “sedimentary rocks of every geologic period from the Cambrian through the Tertiary,” (Carlson and Anderson, 1965) and reflects the sequence subdivision created by Sloss (1963). The structure is described as a large intracratonic basin that shows evidence of initial subsidence during the Ordovician as well as an abnormally complete rock record (Heck et al., 2002). There are six major unconformities found in the cratonic interior of North America that reflect a period of regression maxima (Sloss, 1963). The six subdivisions are as follows; the late Precambrian (the Sauk sequence), the early Middle Ordovician (the Tippecanoe sequence), the early Middle Devonian (the Kaskasia sequence), the

"Post Elvira" Mississippian (the Absaroka sequence), the early Middle Jurassic (the Zuni Sequence), and the Late Paleocene (the Tejas sequence) (Sloss, 1963). The lithology, fluid phase, fluid chemistry, reservoir temperature, pore geometry and other geological factors are examined in order to characterize geothermal wells (Sanyal et al., 1979). The Williston Basin is, by Sanyal's standards, a low to moderate temperature, sedimentary basin of low to moderate salinity.

CHAPTER II

METHODS

Temperature Correction and Reservoir Estimation

Prior work on the feasibility of using GIS for site selection

Publicly available data on magnetic, gravity, lineaments, and earthquakes in a GIS assessment of five sites in Turkey was used to examine geothermal potential (Tufekci et al., 2010). Four evidence maps were created which were then used to predict potentially economically productive sites for geothermal power productions; an epicenter density map, a distance to lineament map, a distance to major graben map, and a magnetic anomaly map. The epicenter density map was used to determine areas with high permeability and water convection, the distance to lineament map was used to determine where water could convect downwards to become heated, the distance to major graben map was used to identify areas of higher geothermal gradients, and the magnetic anomaly map was used to determine local rock assemblages. Two of the sites identified as potentially productive by this method were the two sites already being exploited, which gave credence to the study.

Bottom-Hole Temperature Corrections

Oil wells are typically drilled with the aid of a drilling mud, which heats the near-surface rock or cools the deeper rock within the well. Therefore, recorded bottom-hole temperatures are not at equilibrium and must be corrected. A method by which bottom-hole temperatures could be corrected to be closer to equilibrium values was created by Harrison et al. (1983). The best bottom-hole temperatures are obtained from pressure

tests done in air drilled gas wells, since these wells do not use a circulating mud that can alter the temperature of the well fluid. The problem, however, is that air drilled well data is not as widely available as temperature data from drill stem tests done when the oil wells are first drilled.

Temperature data from the Arkoma and Anadarko basins was used to determine a best fit line to be used for corrections (Figure 4) (Harrison et al., 1983). Blackwell and Richards (2004) converted Harrison's work into metric units and calculated the following equation:

$$Tcf = -16.51213476 + 0.01826842109 \cdot Z - 2.344936959 \cdot 10^{-6} \cdot Z^2$$

In this equation, Z is depth of the well in meters, and the temperature correction factor (Tcf) in degrees Celsius is then added to existing temperature measurement.

The American Association of Petroleum Geologists (AAPG) Geothermal Survey of North America (GSNA) data was obtained by Blackwell and Richards (2004), to which the Harrison correction was applied, determining that even after this correction the results of the corrected logs did not match the data collected from logs of wells at equilibrium. They proposed the following additional correction, known as the SMU (Southern Methodist University) correction: "For wells with gradients of less than 20°C/km (Celsius per kilometer) no change was made. (The) wells with gradients between 20-26°C/km tended to have temperatures too high, thus up to 5°C was subtracted. From 27- 31°C/km the gradients were too low so values were added to the corrected BHTs respectively from 2-10°C. Gradients over 30°C/km had a constant value of 11°C added to the temperature. (Blackwell and Richards, 2004b)" Figure 5 shows the results of these corrections for one of the wells in their dataset.

Temperature Correction in the Williston Basin

I obtained uncorrected bottom-hole temperatures (Figures 6, 9) (LeFever, Personal communication) for the purpose of identifying potential geothermal resources within the Williston basin. These wells are mud-drilled oil wells, thus a correction has to be calculated to ensure the identification of realistic locations for a binary power plant. First, the Harrison correction was calculated for the bottom-hole temperatures and plotted (Figure 7), then the SMU correction was applied (Figure 8). The scatterplots show that the Harrison equation is the best fit for the data analyzed, with the SMU correction showing a larger scatter in the plot.

I applied a method of integration on the best fit lines obtained from plotting the data on a chart within an excel spreadsheet to determine which correction attempt had a smaller area between curves. I also calculated the standard deviation for each set of corrected data. The concept is that the integration with the smallest area between curves while still having the smallest standard deviation would be the most accurate correction. The X-axis of the graph is depth in meters, and the Y-axis of the graph is in degrees Celsius, therefore I defined the unit of integration as degree meters. The integration of the curves for the uncorrected data and the Harrison correction yielded an area value of 42,932.4 degree meters with a standard deviation of 34.0°C. Integrating the curves for the uncorrected data and the SMU correction gave an area value of 56,910.37 degree meters and a standard deviation of 35.98°C. With the smaller area and smaller standard

deviation, it appears that the Harrison correction alone is the most accurate correction of the two for the Williston Basin.

Reservoir estimation within the Williston Basin

I used GIS techniques, after Yang and Xu (2010), to calculate the position of the water and then calculated the volume of each reservoir. The method of using average thickness along with the area containing an appropriate temperature can, therefore, yield a reasonable and useable estimate of a reservoir within the Williston Basin.

Ten reservoirs were selected for having bottom-hole temperatures greater than 90°C within the sedimentary Williston Basin in North Dakota. I created a GIS geodatabase using existing bottom-hole temperature and formation thickness data that was archived by Dr. Richard LeFever (personal communication). With the BHT data, estimated reservoir area was calculated for each formation. The resulting number, combined with the formation thickness, was used to calculate an estimate of reservoir volume.

I imported two spreadsheet files into a geodatabase with ArcGIS. The first contained the depth of formation tops in meters, well API (American Petroleum Institute) number, latitude and longitude of the well, and the calculated thicknesses of each formation in meters. The second file contained the BHT in degrees Celsius, state identification number of the well, latitude and longitude, and the total depth of the well. I then created two data plots: a plot to describe the locations of the wells with BHT data (Figure 10), and a plot to describe the locations of the wells with formation thickness data (Figure 11).

I determined the range of useable temperature from Tester et al. (2006) and by the parameters of the organic Rankine cycle binary power plant being used. The minimum temperature required for this particular binary power plant is 90°C. I then determined which wells that fulfilled the temperature requirement in each formation layer by interpolating the BHT values (example, Figure 12), and calculated the surface area with the polygon tool (example, Figure 13). The polygon for surface area was then projected onto the plot that contained the thickness dataset and we calculated the average thickness within each reservoir area. Standard deviation of both thickness and temperature accuracy were calculated for quality control. I entered these values into a Microsoft Excel spreadsheet to calculate volumes for each formation, at each range of temperatures. A potentially economically productive reservoir was defined as one having at least five wells with a BHT over 90°C within the same formation. The data was plotted using NAD83 (North America Datum, 1983) on an Albers Projection base map.

I calculated the useable energy in each reservoir from $Q = \rho C_p V \Delta T$, where Q is the available heat, ρ is the density of water, C_p is the heat capacity of water, V is the volume of the reservoir, and ΔT is the change of water temperate as it enters and exits the heat exchanger. The following assumptions were made: the density of water at 100 degrees Celsius is 965.3 kg/m³, the heat capacity of water is 4181.3 Joules / (kg * K (Kelvin)), 0.1 % of the total thermal energy contain in the geothermal fluid is the useable amount of energy per year (Sorey et al., 1983), and the temperature of the water as it exits the exchanger was decreased to 50°C.

Creating the Geodatabase

To determine geothermal power plant placement using a geodatabase, several parameters needed to be defined. Co-produced fluids of 100°C are required for power production (Tester et al., 2006), but modern binary power plants can produce power with temperatures as low as 90°C. Conditions appropriate for the placement of cooling towers were considered, but with the local annual temperatures being so low (approximately 10°C annually), air cooled towers were determined to be sufficient. The last parameter necessary for placement of a plant was the consideration of well water flow rate. The Williston Basin does not have a large volume of fluid flow, so an appropriate number of closely spaced wells, determined by the local flow rate, are required to provide the needed amount of flow. Once the parameters of the project were defined, it was possible to create the necessary spreadsheets in Microsoft Excel and import them into ArcGIS for data analysis.

Gathering the Data

The Well Index file from the North Dakota Geological Survey Oil and Gas Subscription Service was downloaded and imported into ArcGIS for the purpose of obtaining well ownership, well status, and the latitude and longitude of every well in the state of North Dakota. A second Microsoft Excel spreadsheet, the aforementioned dataset obtained from Dr. Richard LeFever (Personal Communication), had BHT data for over 10,000 wells within the Williston Basin. The third Microsoft Excel spreadsheet was created with data that was obtained from the North Dakota Geological Survey Oil and Gas Subscription Service with BBL water production from active wells in January 1985 and July 2010. The 1985 date was chosen because the data from Dr. LeFever's BHT file was compiled from wells active in the mid-1980s, and the 2010 date was chosen because

a modern analog was necessary. In addition, the BHT data set was supplemented by using Optical Character Recognition (OCR) on original scout files from the North Dakota Geological Survey Oil and Gas Subscription.

Analyzing the Data

With the geodatabase in place, it was then possible to plot a series of maps by formation, to provide depth data, as a consideration for the cost of future water pumping. All wells in each formation with a BHT greater than 90°C were located as the first step in data analysis. All of the datasets were then combined to isolate all wells with a BHT greater than 90°C to further isolate the wells to find clusters of at least five wells per location for the purposes of achieving appropriate flow rates.

CHAPTER III

RESULTS

Overview

The dataset includes 10,955 wells with BHT data, 2,899 wells with production data from January 1985, and 1,657 wells with production data from July 2010. The BHT analysis yielded ten formations of sufficient temperature with sufficient locations for piggy-backing a small power plant on producing oil field structures for oil field power use, and many more dry well locations that had sufficiently high water flow for a larger, commercial power plant. I estimated the useable thermal energy of selected oil-producing formations that have temperatures in a range from 90°C to more than 150°C in the Williston Basin. I determined the total solid rock volume of ten reservoirs which were grouped by system from Pennsylvanian to Cambrian, and estimated the reservoir size of each of the following temperature ranges; 90°-100°C, 100°-110°C, 110°-120°C, 120°-130°C, 130°-140°C, 140°-150°C, and 150°C and up. The geothermal fluid reservoir volume was calculated using porosity data from the North Dakota Geological Survey Wilson M. Laird Core Library. I assumed a heat exchanger exit temperature of 50°C, meaning that the water lost 40° to 100°C in the process. A recovery factor of 0.1% of the total thermal energy, per year, is appropriate for a sedimentary basin the size of the Williston Basin (Sorey et al., 1982).

The Formations

Pennsylvanian: Tyler formation:

The Tyler formation (Figures 14, 15 and 16) has an area of 2051.1 km², an average thickness of 0.048 km. The total rock volume was calculated at 95.79 km³. The porosity is 2.7%, and the water volume is 2.7 km³. The average temperature of this reservoir is 93.7°C, and the total thermal energy of this reservoir is listed in Table 1.

Of the wells that I had BHT data for, there are ninety-one wells with a temperature of 90°C or higher, and two locations which may be feasible for the placement of binary power plants; one plant may be located along the I-94 corridor, and the other location is located just to the south of the I-94 group.

Mississippian: Heath, Otter, Kibbey, Charles, Mission Canyon, and Lodgepole formations:

These formations (Figures 17, 18 and 19) encompass an area of 35,751.1 km², have a combined average thickness of 0.702 km, and an approximate rock volume for the total reservoir of 20,186.8 km³. The porosity is 3.0% (Otter) and 5.5% (other Mississippian formations), and the total water volume is 1,166.1 km³. The average BHT was 93.8°C (Otter) and 99.2°C (other Madison). The total thermal energy of this reservoir is listed in Table 1.

Of the wells that I had BHT data for, the Otter formation contains 100 wells with a temperature of 90°C or higher, and while similar in well layout to the Tyler formation, it has three groups of wells that could be ideal locations for binary power plants. The largest grouping of wells is along the I-94 corridor, with another large grouping directly to the south and a smaller grouping to the south west. The plot of the other Madison formations had the largest number of wells (2,270), with a temperature of 90°C or higher. The wells are clustered in multiple spots throughout the state.

Devonian: Bakken, Three Forks, Birdbear, Duperow, Souris River, Dawson Bay, Prairie

Evaporite, Winnipegosis and Ashern formations:

The area of these formations (Figures 20, 21, 22, 23, and 24) is as high as 50,641.4 km², with average thicknesses of 0.018 km (Bakken), 0.047 km (Three Forks) and 0.323 km (other Devonian formations). The total rock volume for all formations is 17,487.9 km³. The porosity is 4.6% (Bakken), 9.6% (Three Forks), and 5.4% (other Devonian formations). The total water volume is 1,064.9 km³. The average BHT is 103.6°C (Bakken), 103.8°C (Three Forks), and 109.3°C (other Devonian formations). The total thermal energy of this reservoir is listed in Table 1.

Of the wells that I had BHT data for, the Bakken formation has 186 wells with a temperature of 90°C or higher. There are two main clusters of wells; a smaller one near I-94 and a large grouping on the western edge of the state. The Three Forks formation has 130 wells with a temperature of 90°C or higher, and is grouped into four small groups and three larger locations that may be ideal for power plant locations. The other Devonian formations have a grouping of 558 wells with a temperature of 90°C or higher that are spread throughout the state.

Silurian: Interlake formation:

This formation (Figures 25, 26, and 27) has an area of 62,566.7 km², an average thickness of 0.174 km, and a rock volume of 10,146.3 km³. The porosity is 6.8%, and the water volume is 740.3 km³. The average BHT is 115.9°C. The total thermal energy of this reservoir is listed in Table 1.

Of the wells that I had BHT data for, the Interlake formation contains 253 wells with a temperature of 90°C or higher, with eight small groupings and three larger groupings. The wells are located mostly along the Missouri River and Lake Sakakawea.

Ordovician: Stonewall, Stony Mountain, Red River, and Winnipeg formations:

These formations (Figure 28, 29, 30, and 31) have an area as high as 71,794.5 km², and average thicknesses of 0.087 km (Winnipeg) and 0.226 km (other Ordovician formations). We calculated the total rock volume at 19,982.3 km³. The porosity is 5.4% (Winnipeg), 5.1% (other Ordovician formations) and the water volume is 1,093.6 km³. The average BHT is 119.0°C (Winnipeg) and 115.3° C (other Ordovician formations). The total thermal energy of this reservoir is listed in Table 1.

Of the wells that I had BHT data for, the Winnipeg formation has fifty-seven wells with a temperature of 90°C or higher. The identified wells are near the Missouri River and Lake Sakacawea with one small group north and one small group south. The plot of the other Ordovician formations have the second largest number of wells with 1,516 at a temperature of 90°C or higher. The wells are located throughout the entire western part of the state.

Cambrian: Deadwood formation:

This formation (Figures 32, 33, and 34) has an area of 66,824.1 km², and an average thickness of 0.085 km, which gives the formation a total rock volume of 5,191.6 km³. The porosity is 8.6 %, and the water volume is 488.5 km³. The average BHT was 120.8°C. The total thermal energy of this reservoir is listed in Table 1.

Of the wells that we had BHT data for, this formation has 120 wells with a temperature of 90 ° C or higher with thirteen small groupings and two large groupings, which are spaced fairly evenly in the western half of the state.

CHAPTER IV

CONCLUSION

Results of the bottom-hole corrections

The uncorrected and Harrison correction integration yielded an area between the curves of 42,932.42 degree meters with a standard deviation of 33.96°C, while the uncorrected and SMU integration gave an area between the curves of 56,910.37 degree meters and a standard deviation of 35.98°C. With the smaller area and smaller standard deviation, it appears that, of the two, the Harrison correction alone is the most accurate for the Williston Basin.

Results of the Reservoir Estimate

The total rock volume of the reservoirs in the Williston Basin, grouped by temperature range, is listed with the total water volume, total thermal energy, and total power availability of the reservoirs in Table 2. The estimated recoverable power based on the range of binary power plant efficiencies is listed in Table 3.

Potential locations for commercial power plants

Areas of high water flow

The water flow data obtained from the North Dakota Geological Survey Oil and Gas Subscription Service was interpolated using the Kriging method. The resultant raster image (Figure 35) indicated several areas with high water flow that could potentially support a commercial grade power plant. The abandoned and dry wells in these areas are

shown in Figure 36. If each area hosted one power plant, there would be ten potentially commercial productive power plant locations within the Williston Basin to choose from.

Summary

Geothermal energy from co-produced fluids is an important economic and underused energy source. The available energy of formation waters in the Williston basin is approximately 7.73×10^{18} Joules, assuming the 0.1% recovery rate from Sorey et al. (1982). A one Megawatt hour (1 MWh) power plant can power 500-1,000 homes per year (Public Service Commission of Wisconsin (PSCWi), 2010). 7.73×10^{18} Joules converts to 2.15×10^9 MWh, enough energy to power 1.075 trillion homes for one year using the smaller number in the range provided by PSCWi. The U.S. Census Bureau lists the projected number of households for 2010 at approximately 80 million. The Williston basin alone has enough available energy to power every household in the United States for the lifespan of the reservoir as a trans-finite resource, as determined by Sorey et al. (1982).

With the low annual temperatures and relatively high heat flow in the Williston Basin, North Dakota is an ideal location for binary power plants. There are ten formations in the Williston Basin with a sufficient number of wells fulfilling the requirements needed for placement of a binary power plant using existing wells.

Using existing wells is much more cost efficient than drilling new wells. Using Tester et al. (2006), the cost of drilling a new oil well was approximately \$1,800/m when the study was done, yet most work-overs that require mobilizing a rig will only cost between \$700,000 and \$1 million, depending on the depth of the well that is being

reworked. The evidence provided proves that geothermal energy in the Williston Basin is underutilized.

APPENDICES

APPENDIX A

Figures

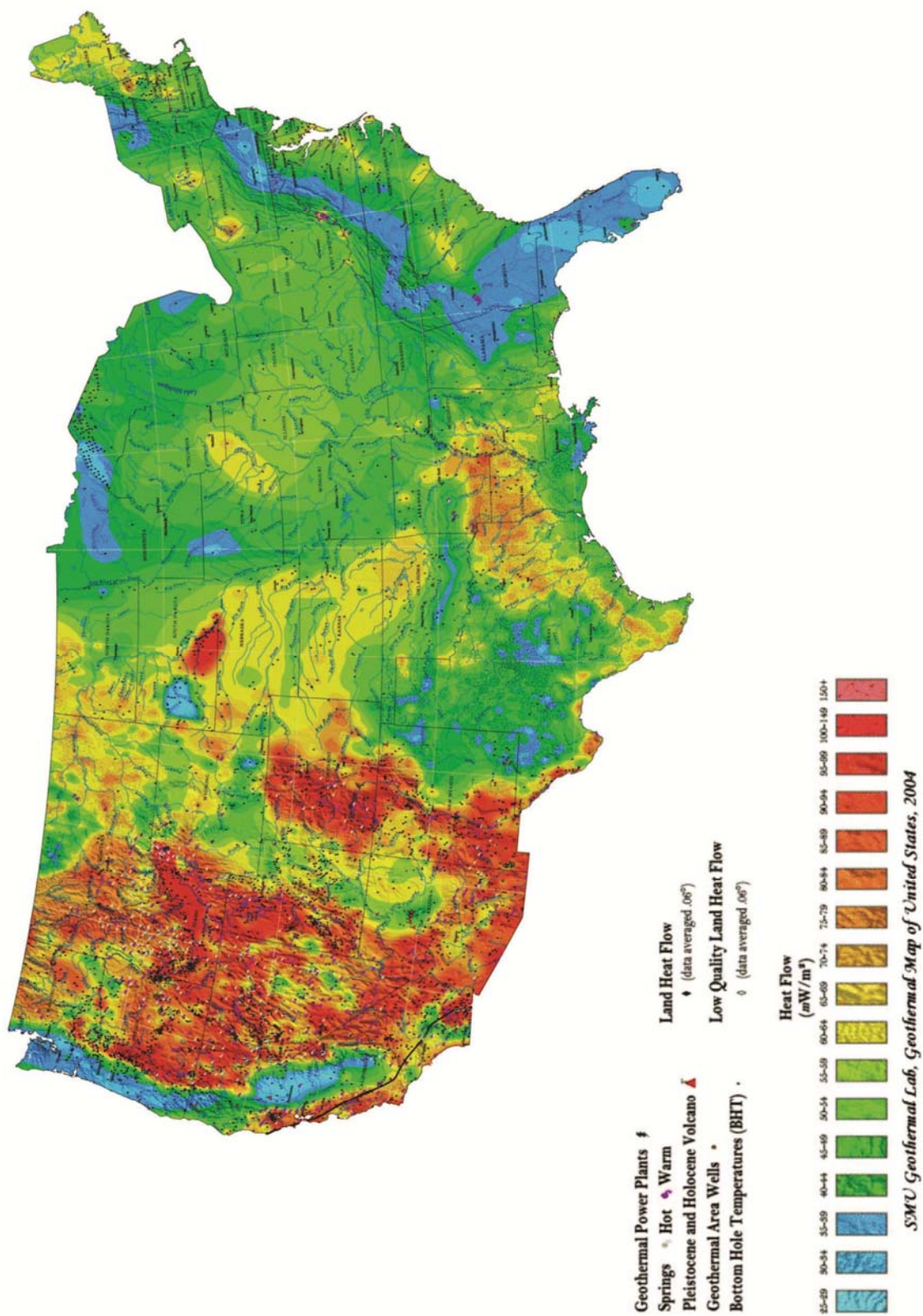


Figure 1 -- The Geothermal Map of United States (Reprinted with Permission, Blackwell and Richards, 2004)

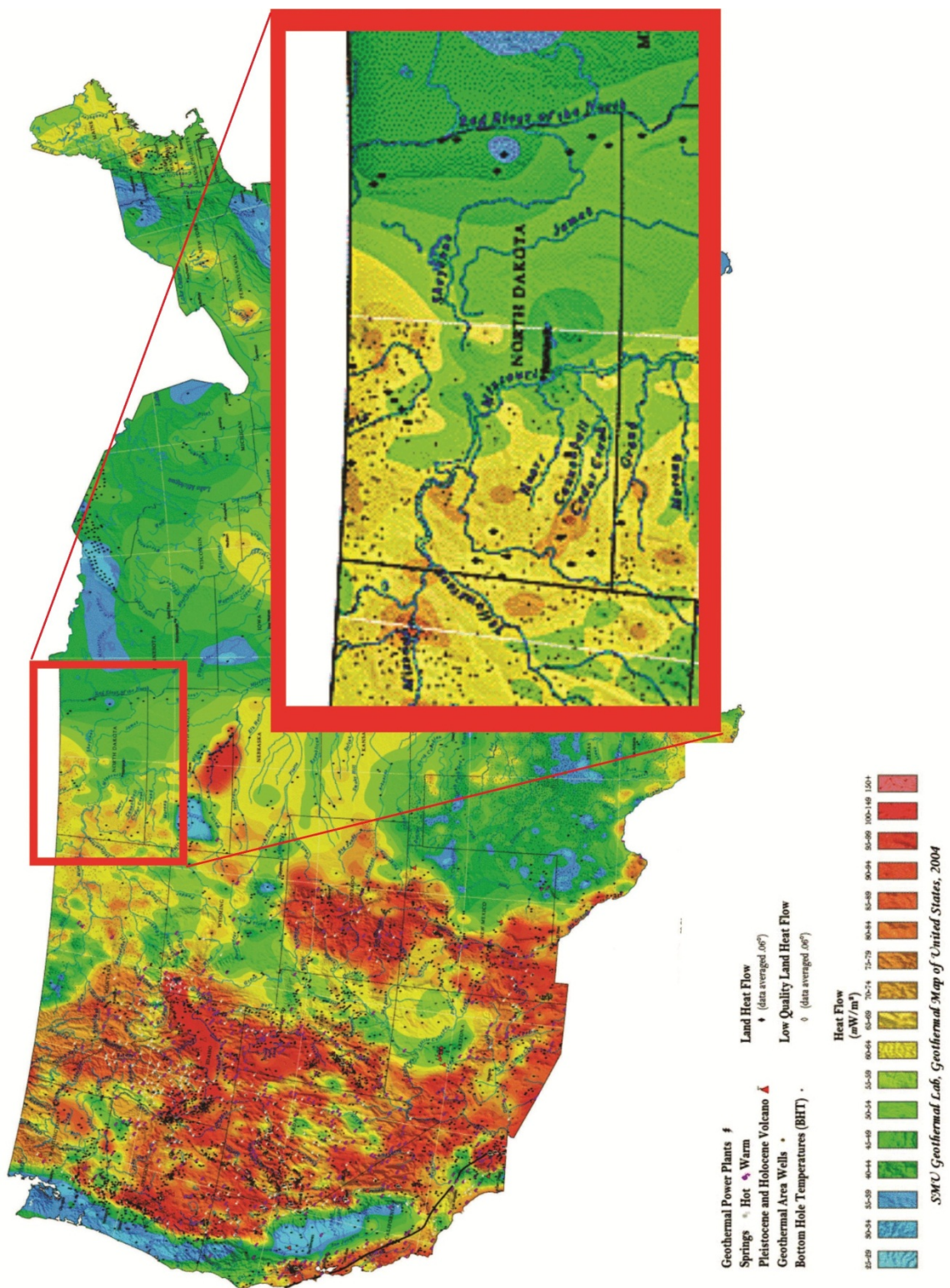


Figure 2 -- Inset of the Geothermal Map of the United States showing Williston Basin detail (Modified from Blackwell and Richards, 2004)

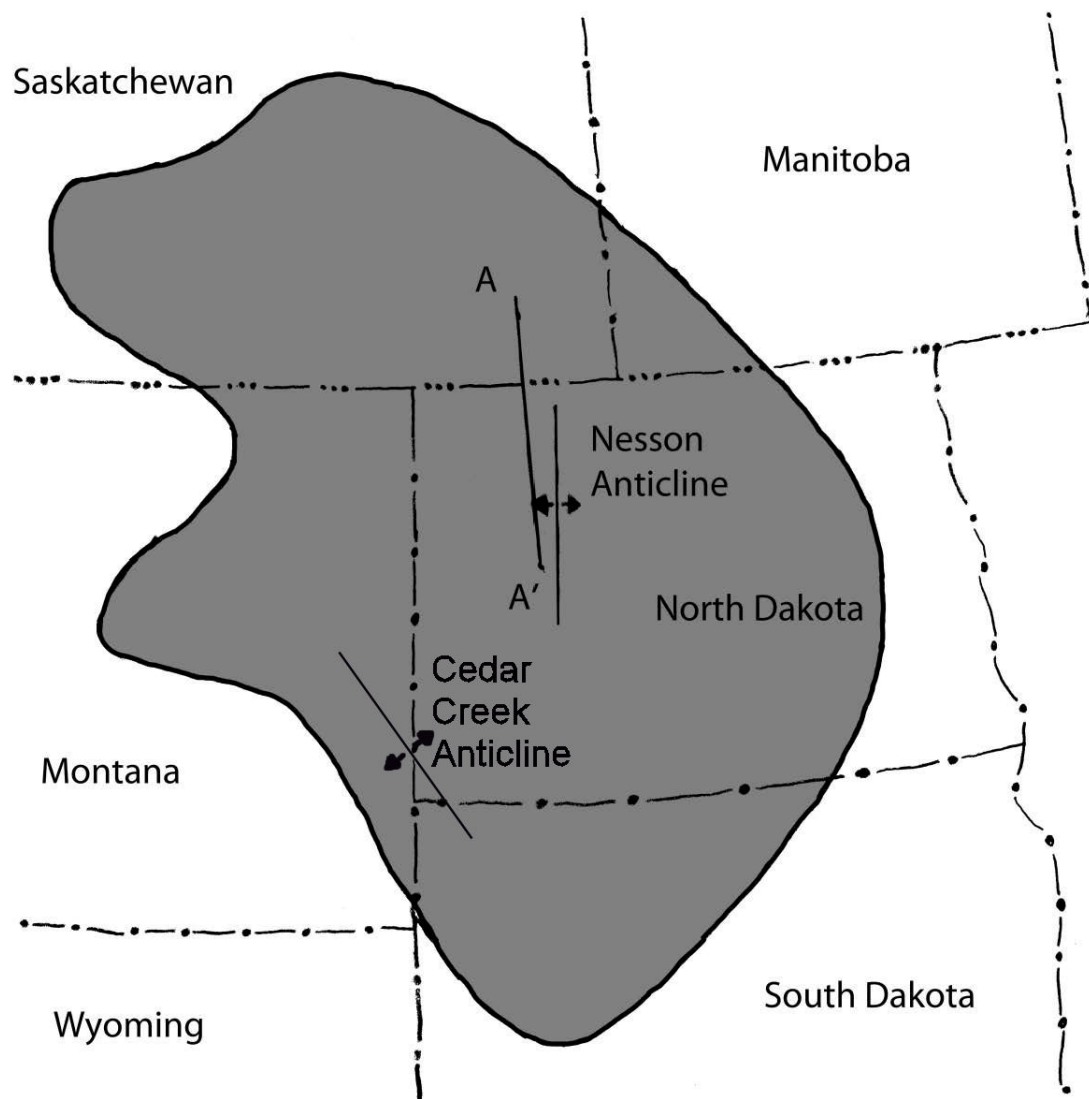


Figure 3 -- The Williston Basin, showing the Nesson and Cedar Creek Anticlines.
(Modified from Heck et.al., 2000)

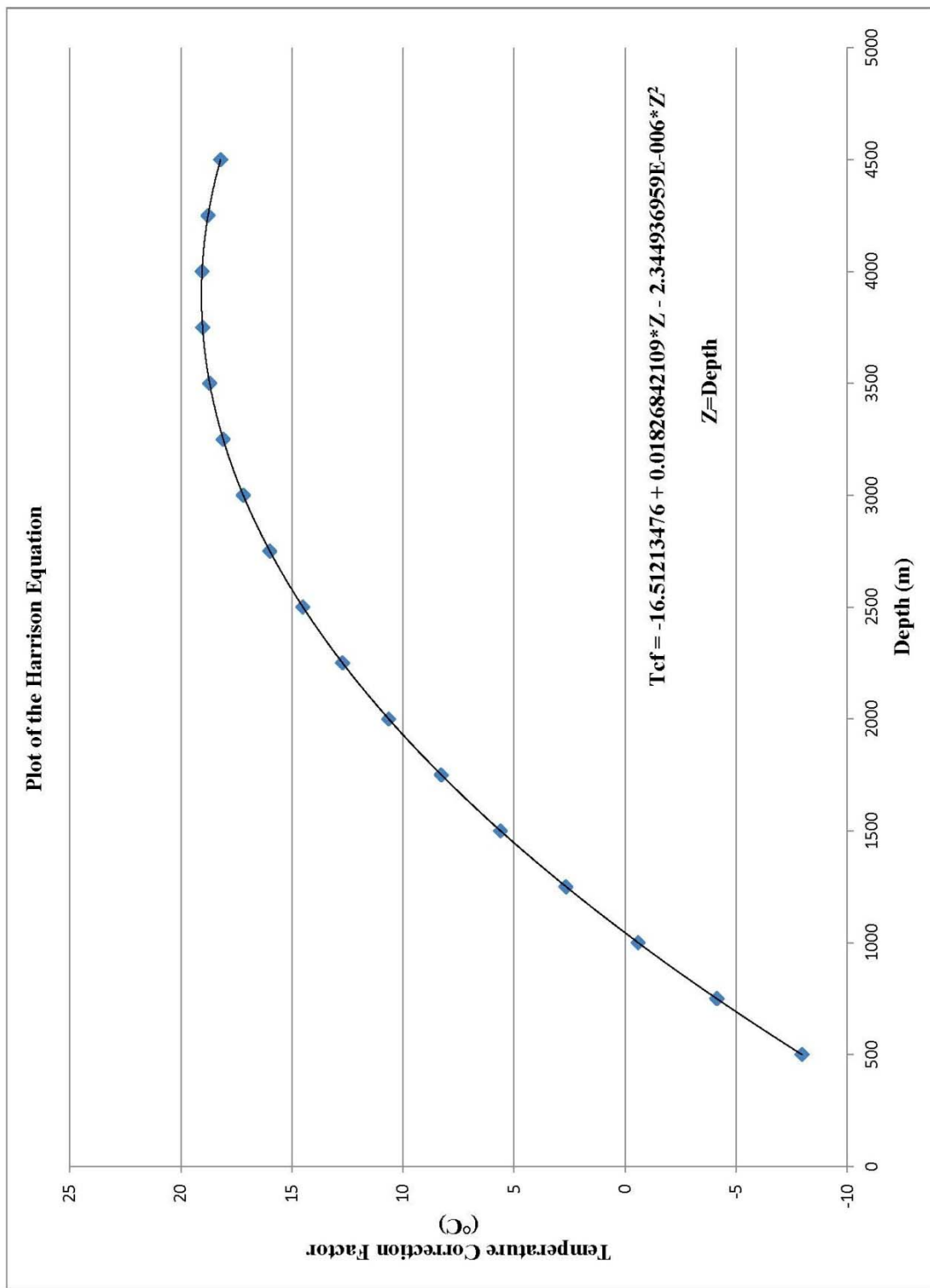
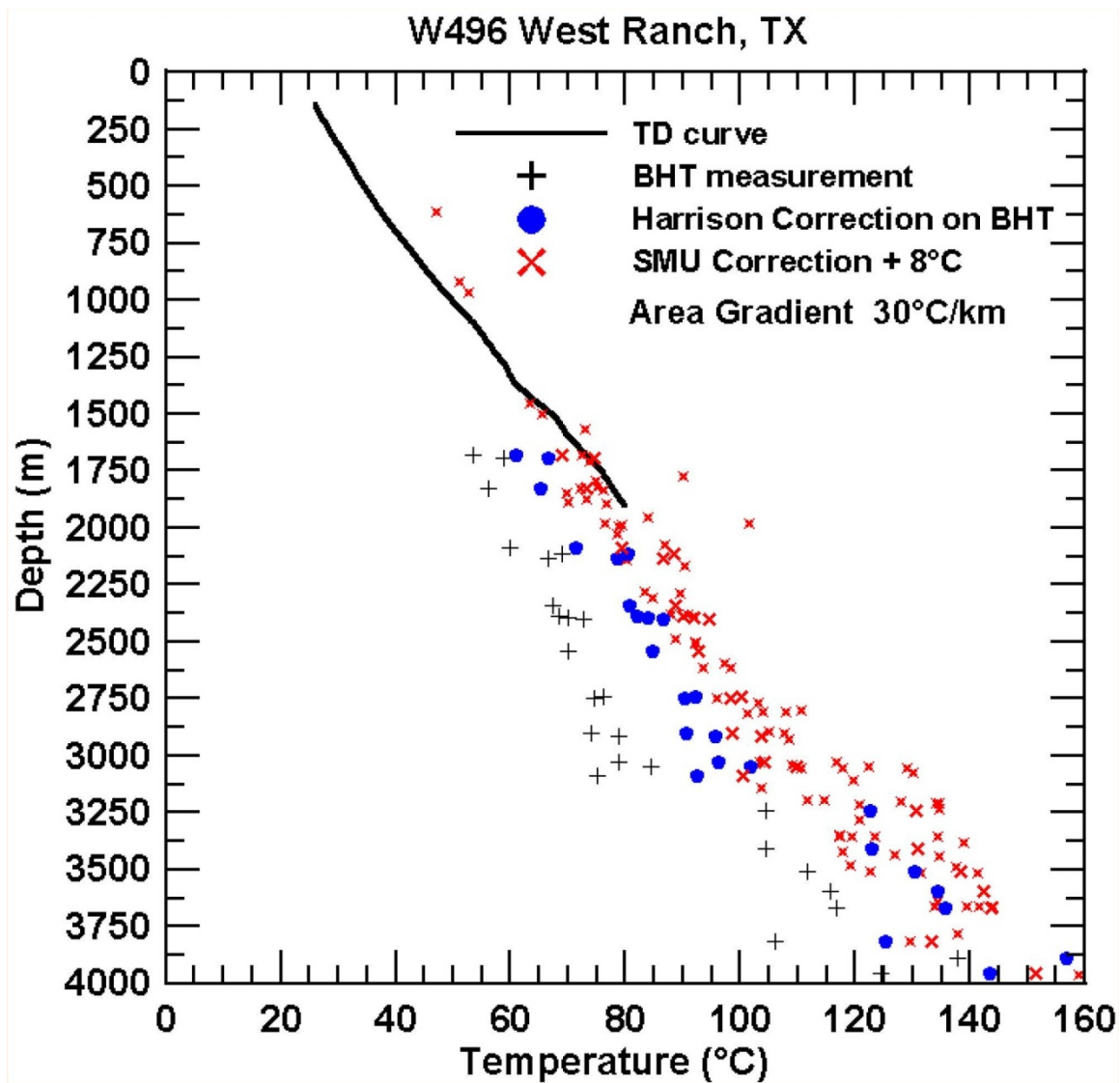


Figure 4 -- Graph of the Harrison Equation (Equation from Blackwell and Richards, 2004)



**Figure 5 -- Temperature/Depth (TD) Plot from Blackwell and Richards, 2004a.
(Reprinted with Permission)**

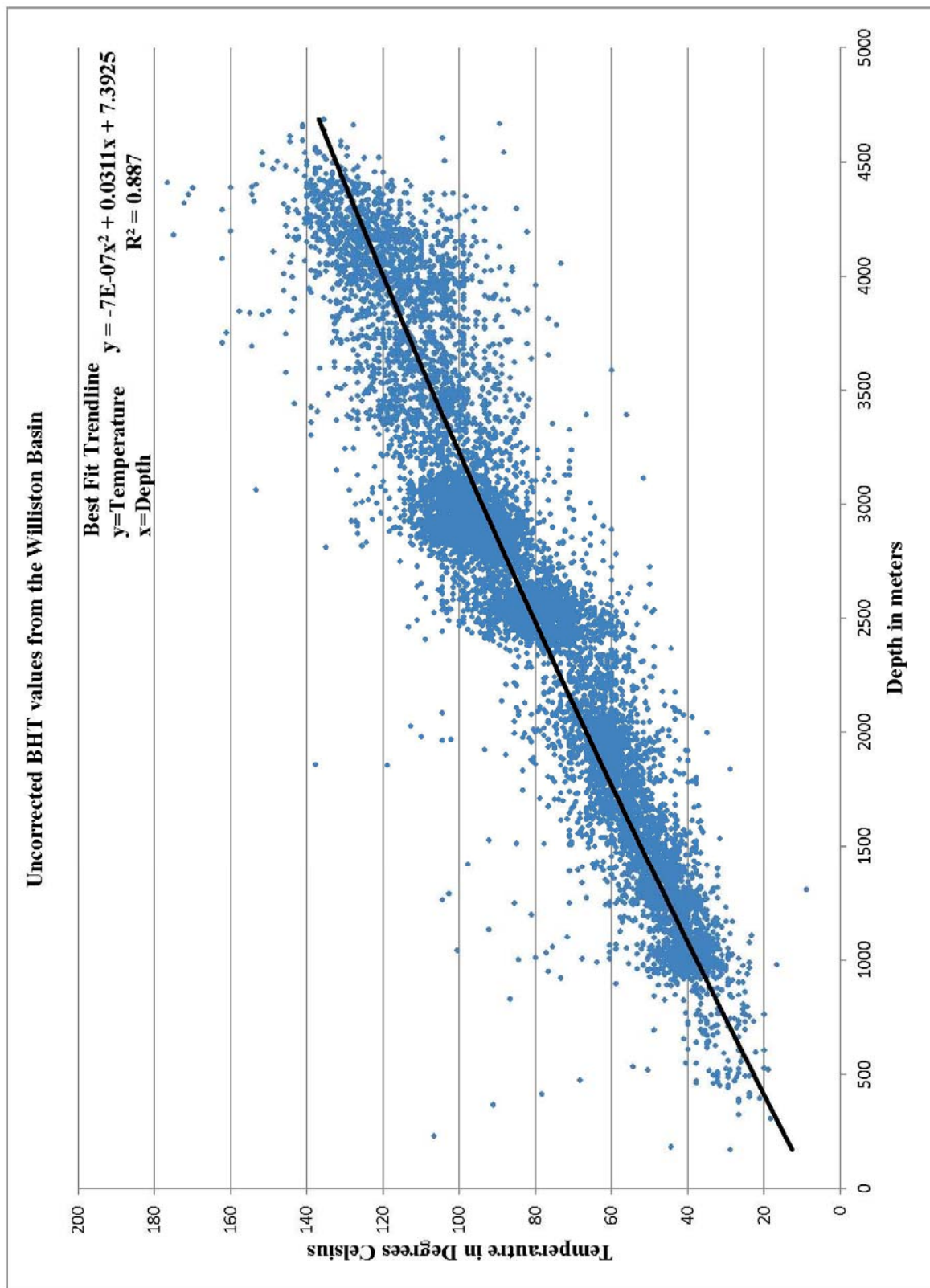


Figure 6 - Graph of Uncorrected BHT Values

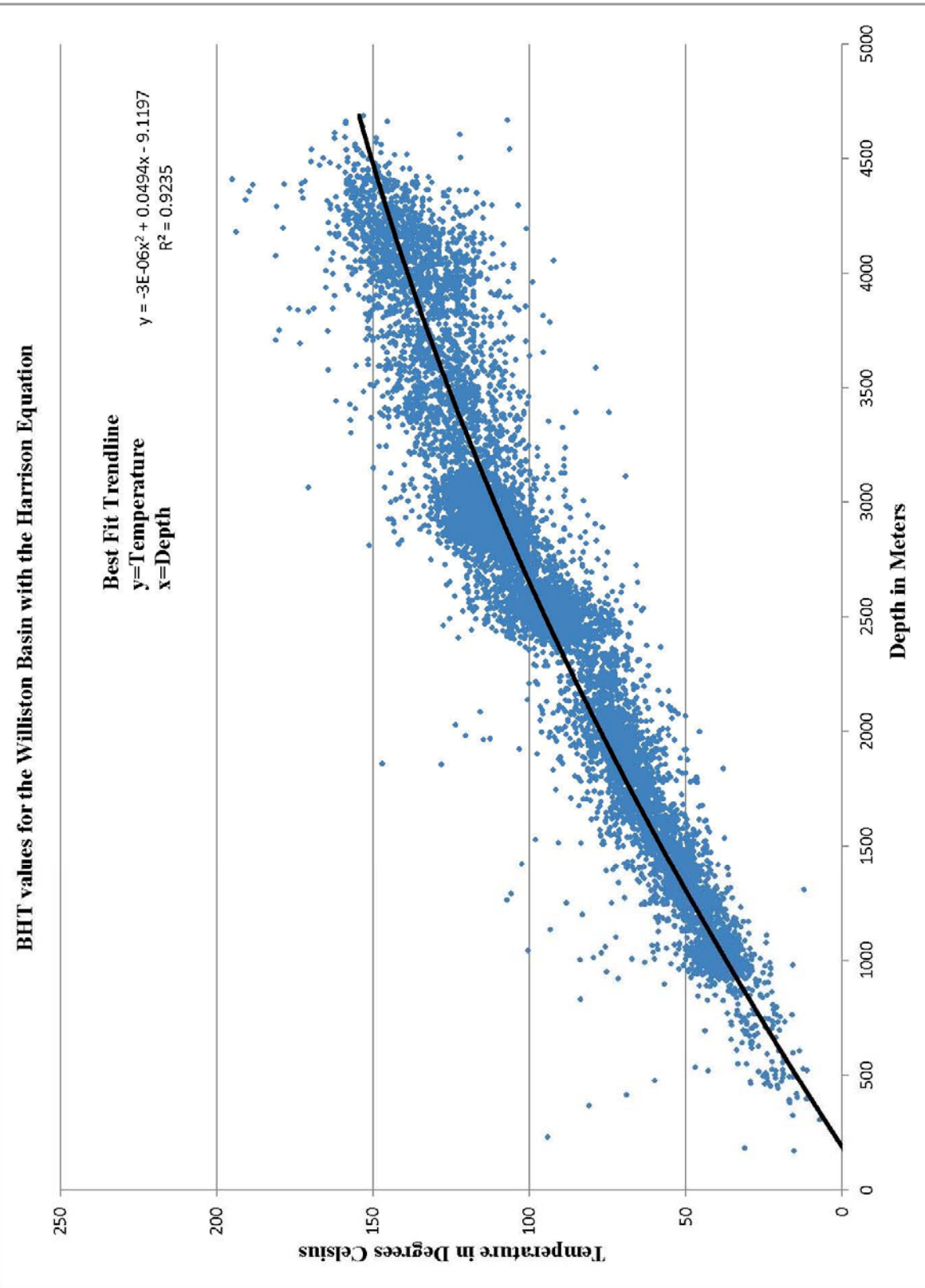


Figure 7 -- Graph of BHT Values after the Harrison Correction

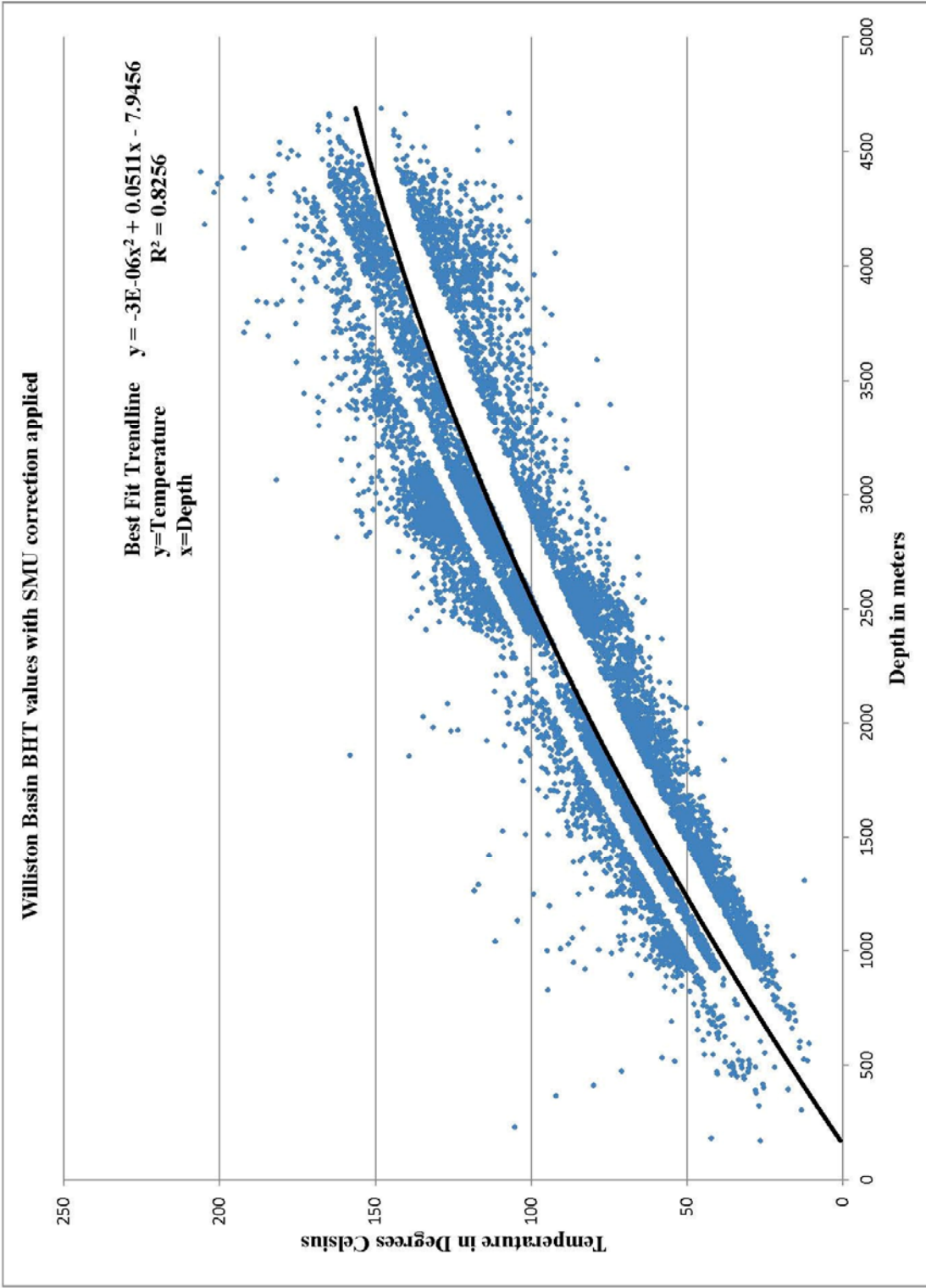


Figure 8 -- Graph of BHT values after SMU Correction. The blank areas are a result of the correction method and may be caused by an inaccurate estimate of the local geothermal gradient.

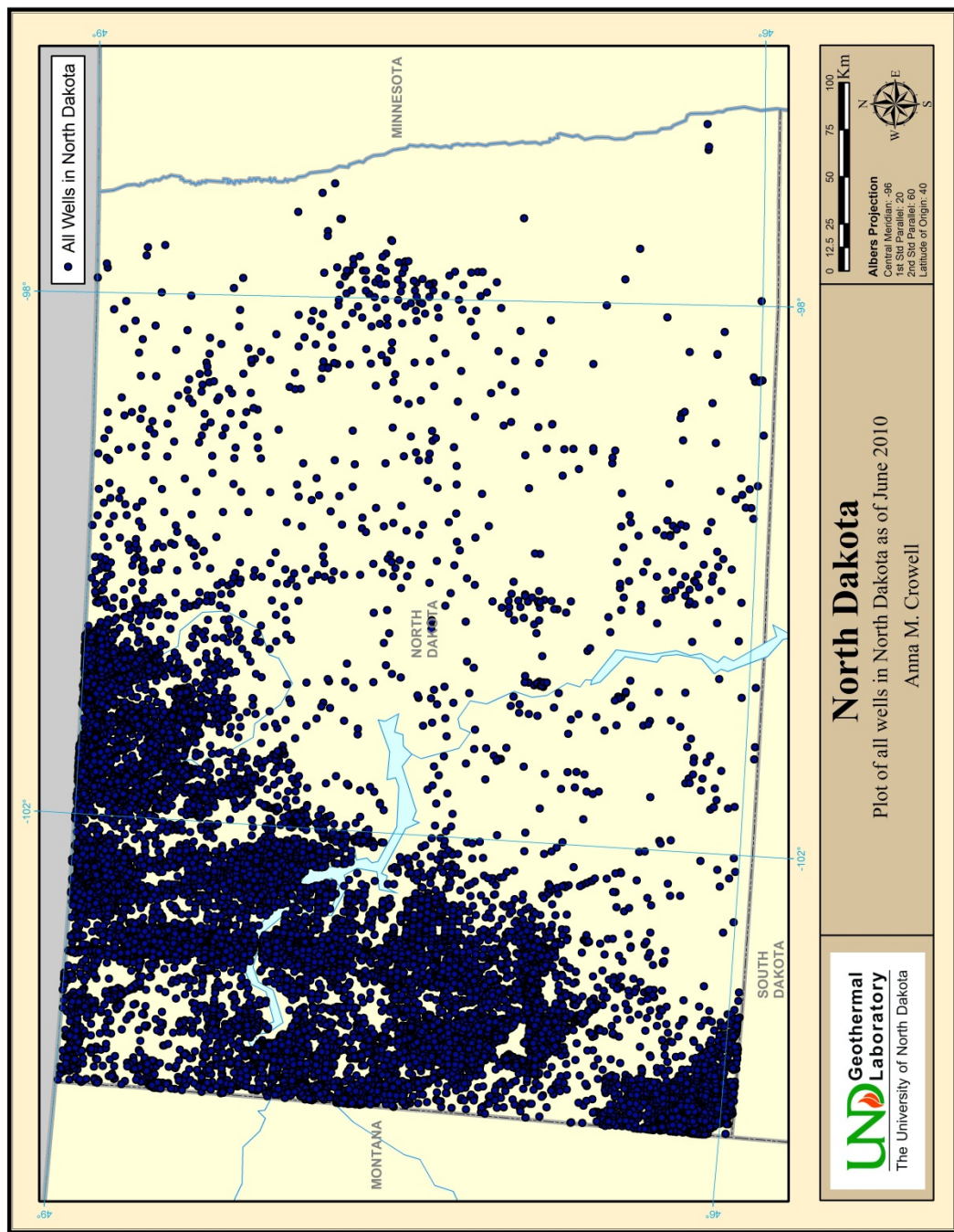


Figure 9 -- Plot of All Wells in North Dakota, as of June 2010

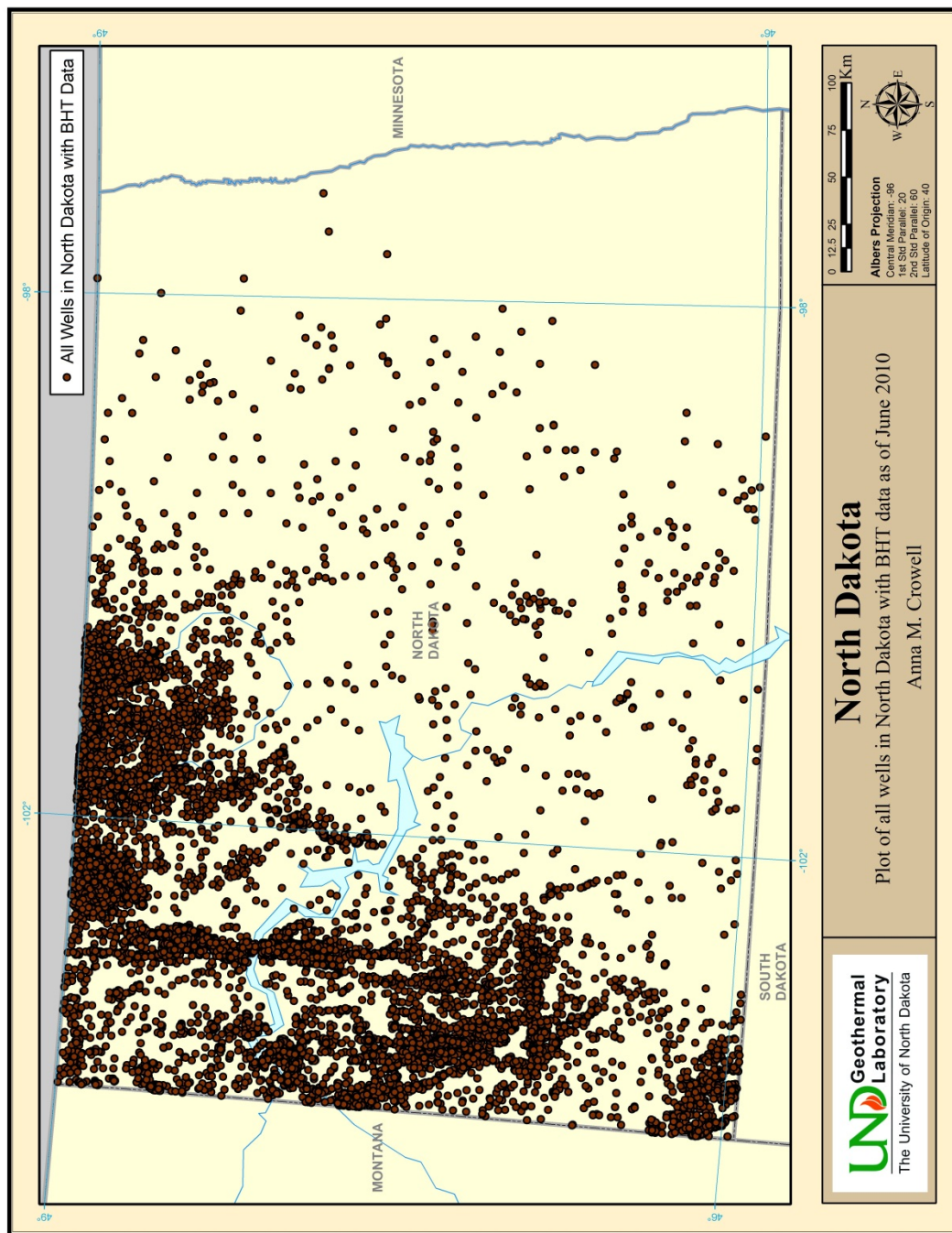


Figure 10 -- Plot of all wells in North Dakota with BHT data

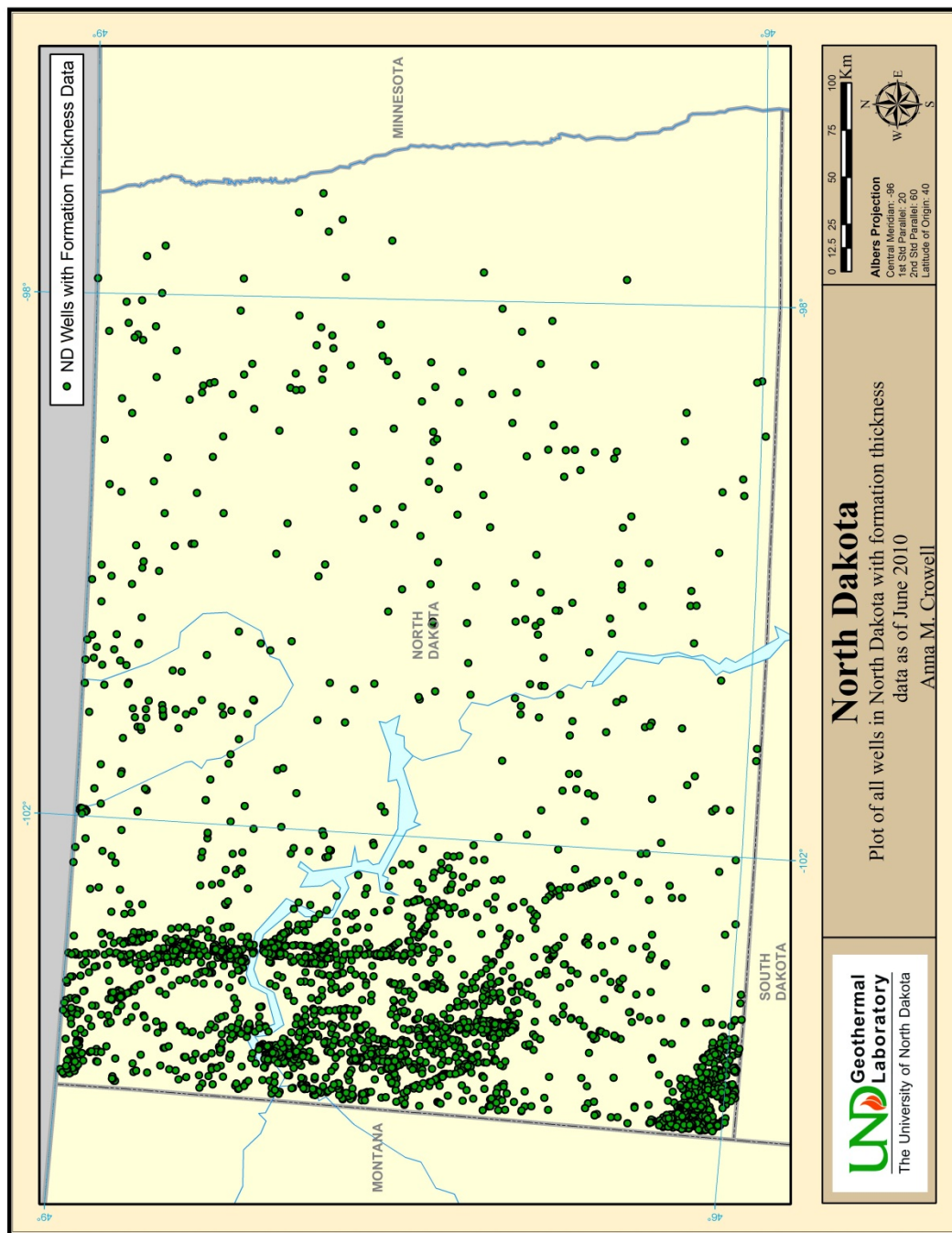


Figure 11 -- Plot of all wells in North Dakota with formation thickness data

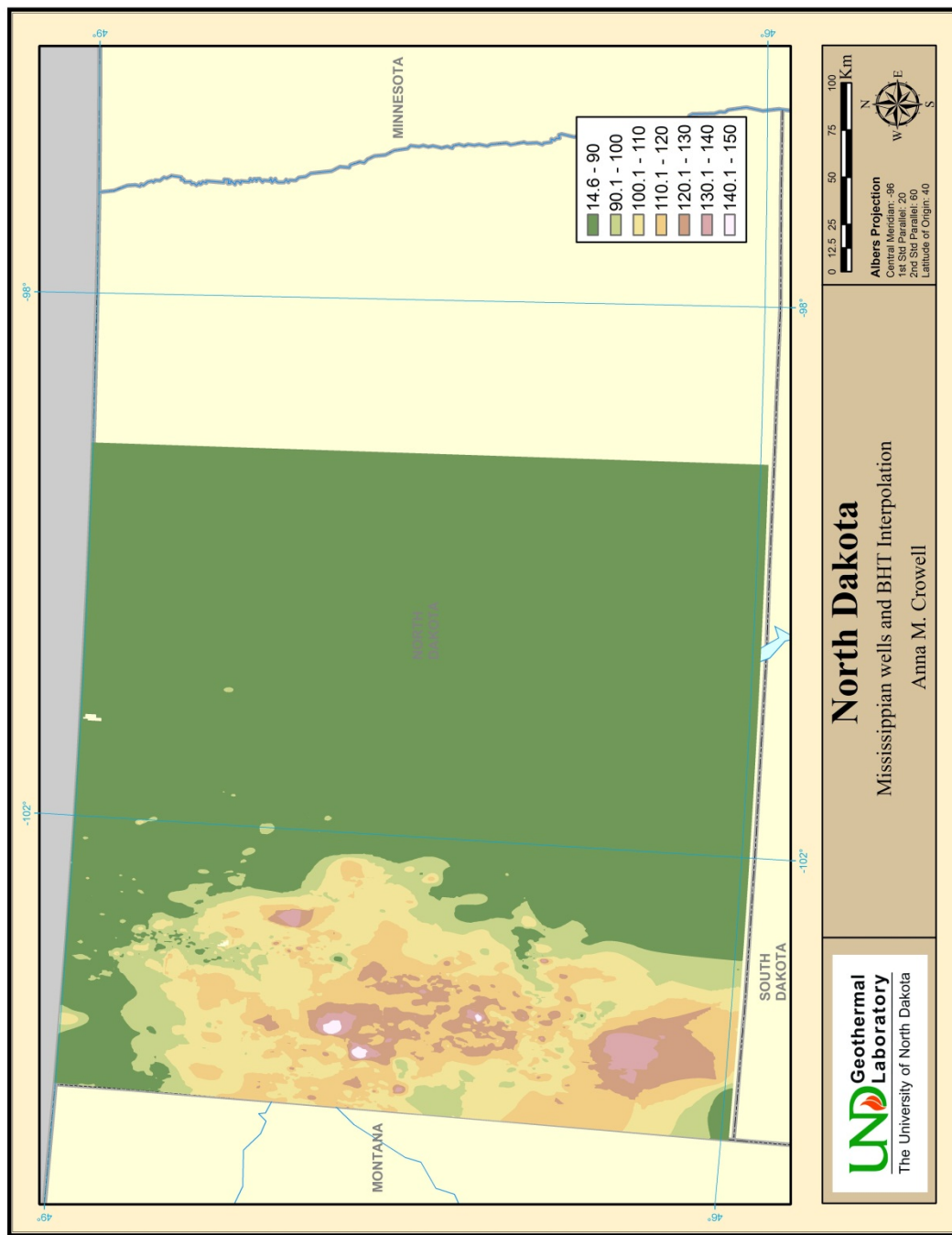


Figure 12 -- Example of BHT Interpolation

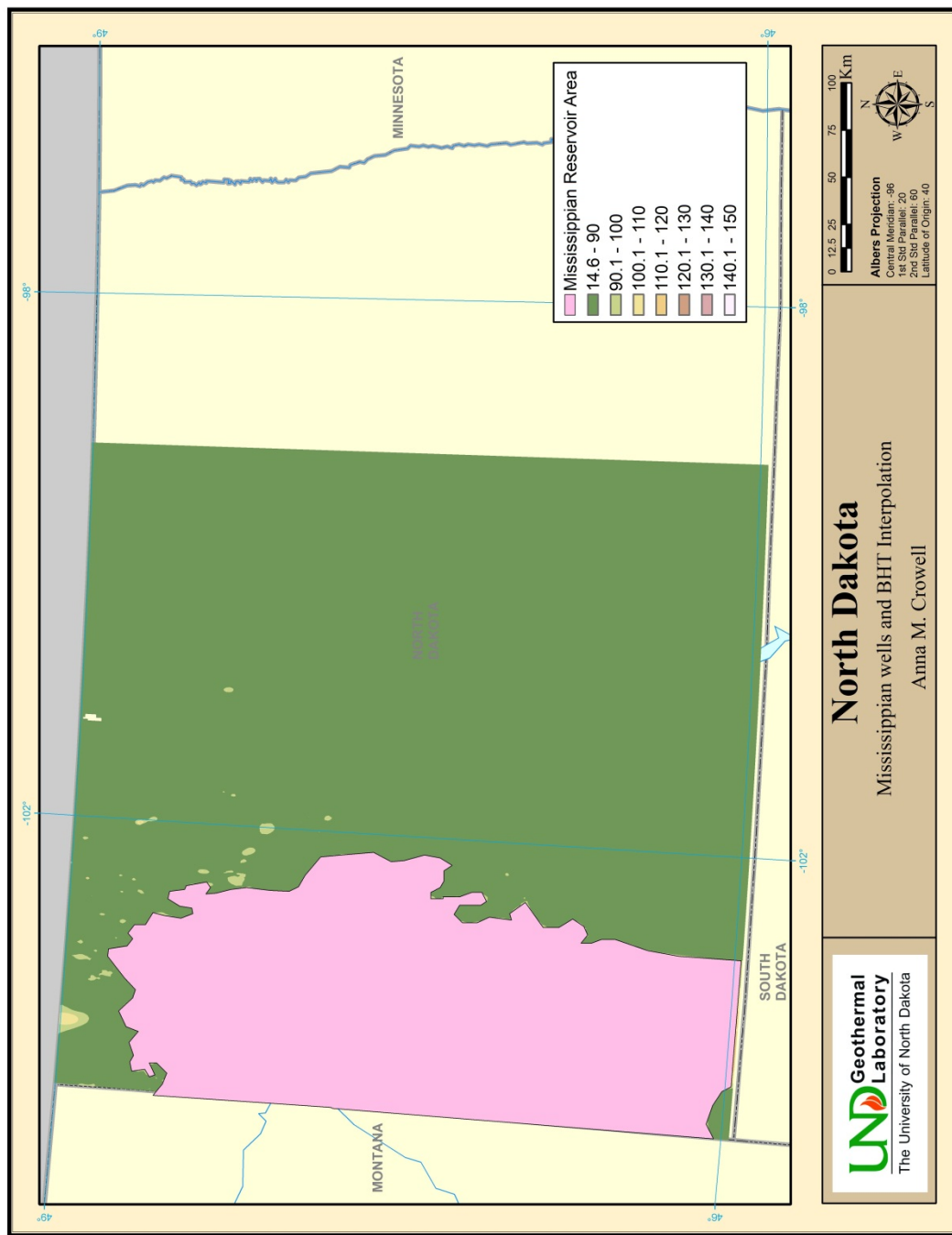


Figure 13 -- Example of polygon used to determine area

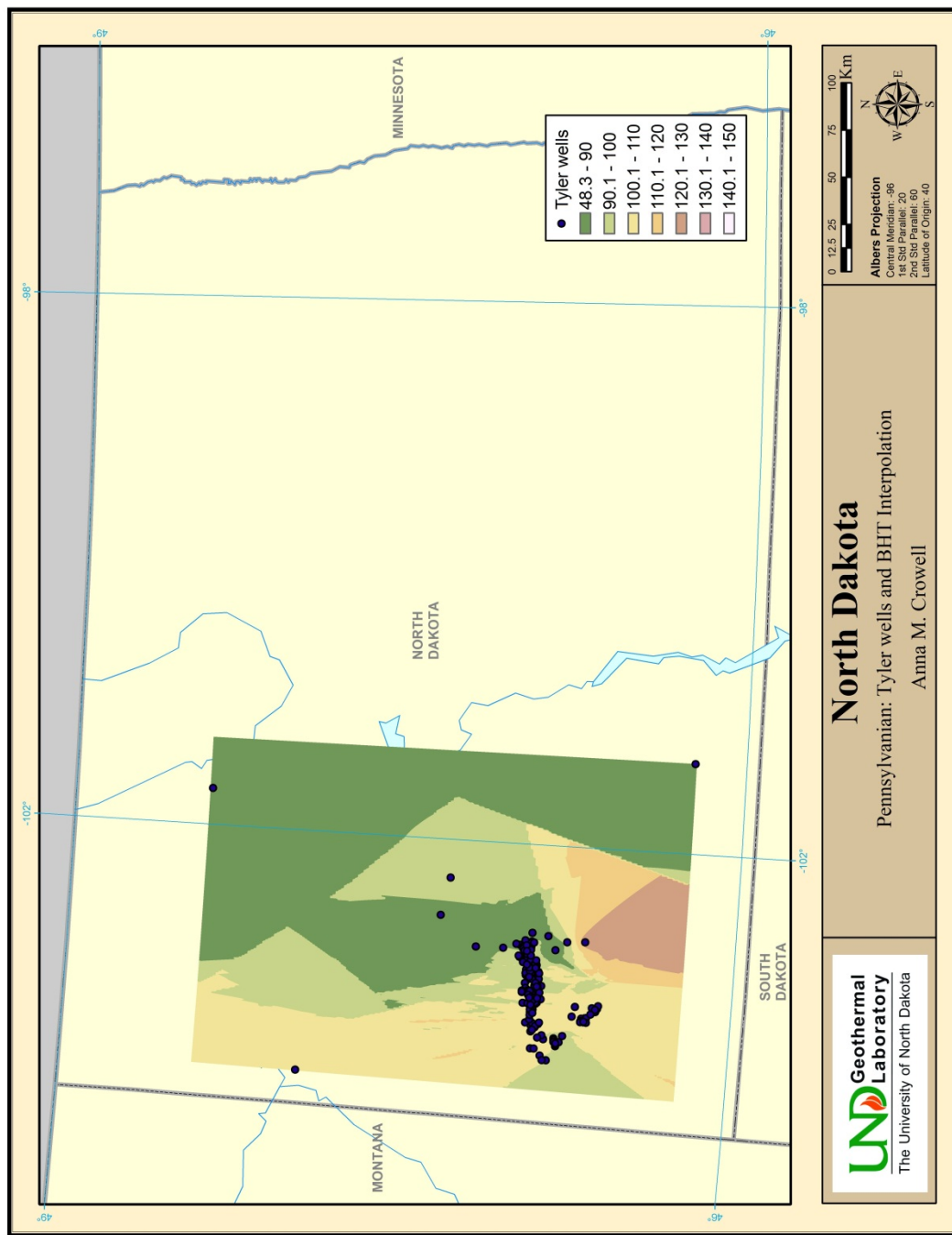


Figure 14 -- Estimate of the reservoir area in the Tyler formation

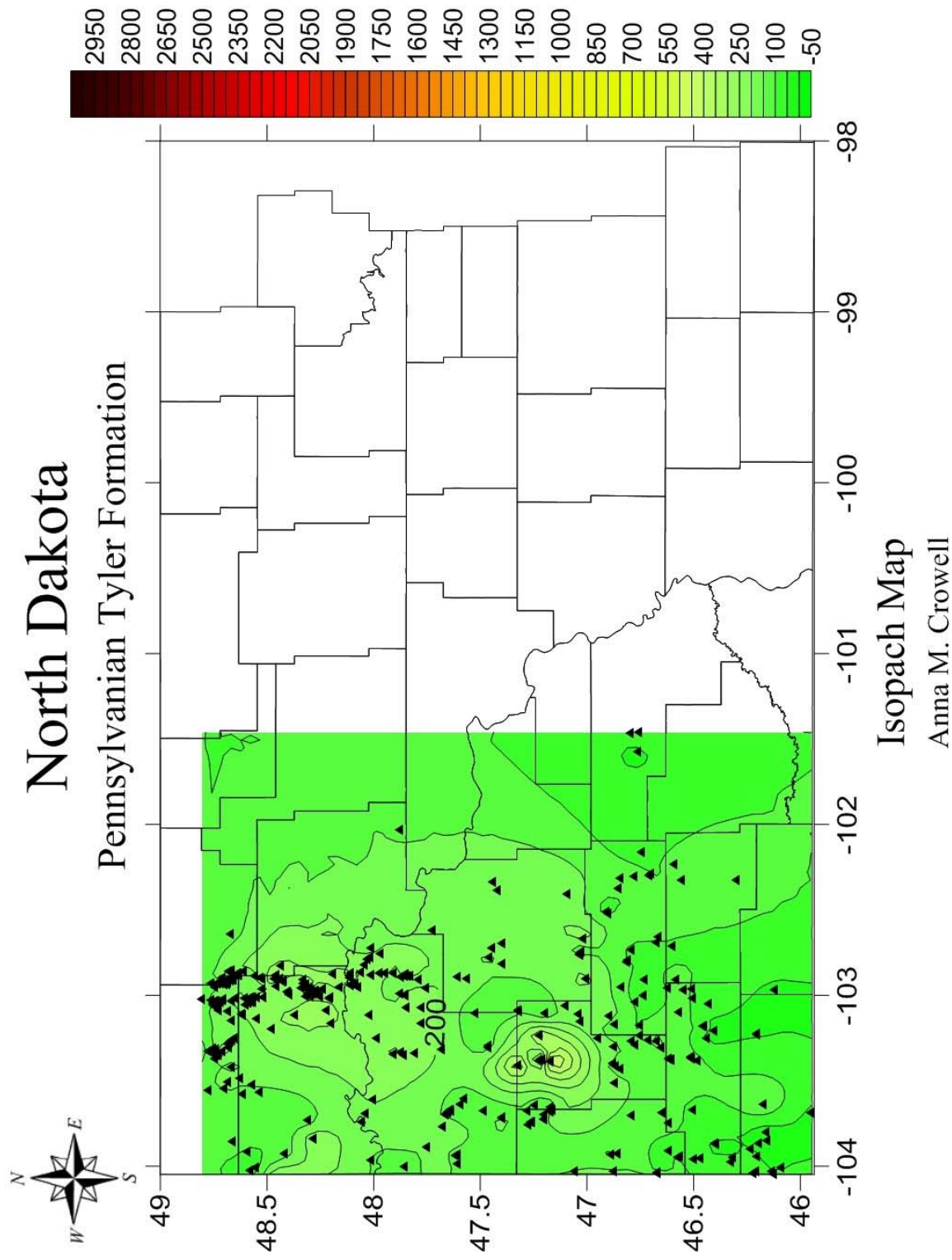


Figure 15 -- Isopach map of the Pennsylvanian Tyler formation

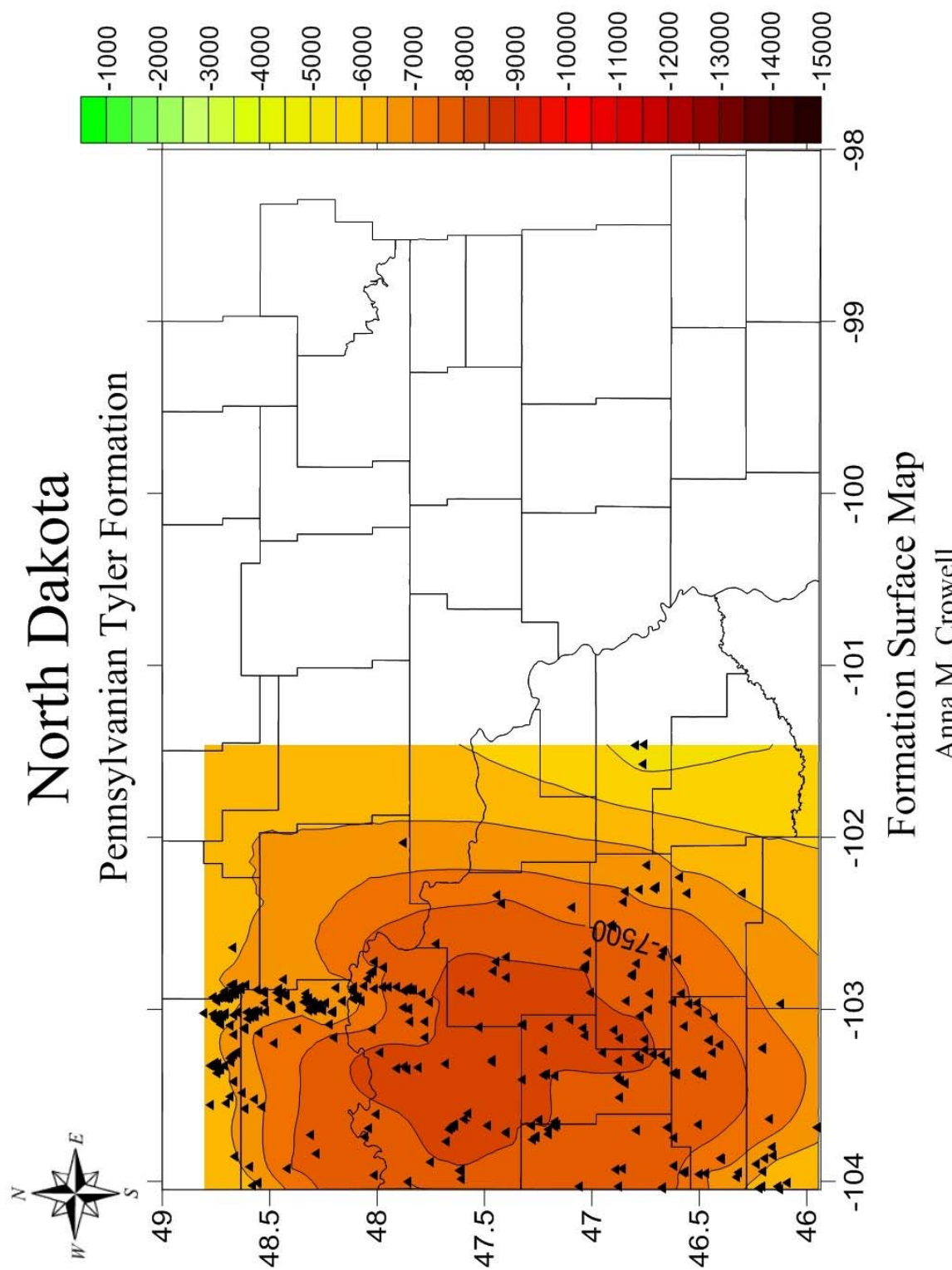


Figure 16 -- Formation surface map of the Pennsylvanian Tyler formation

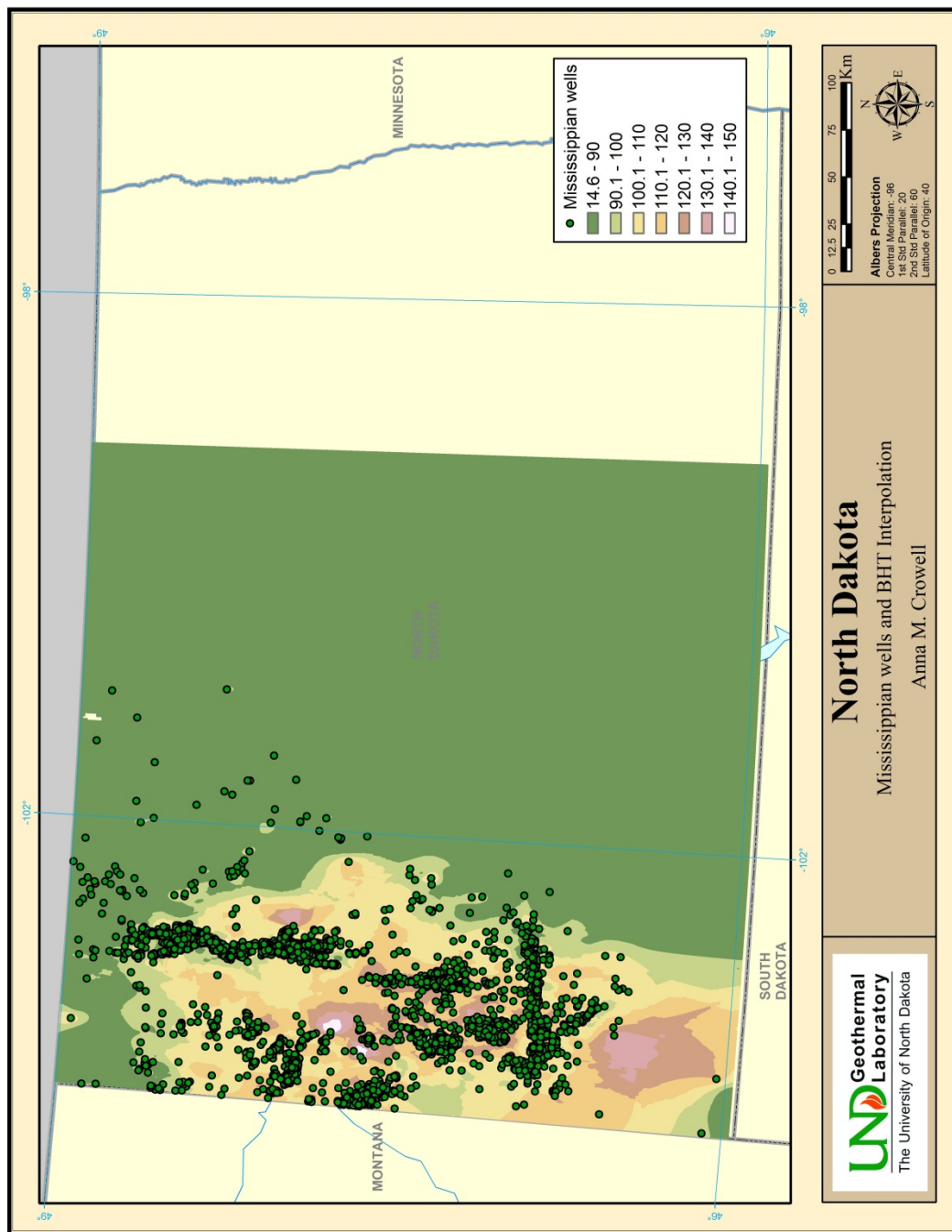


Figure 17 -- Estimate of the reservoir area in the Mississippian formations

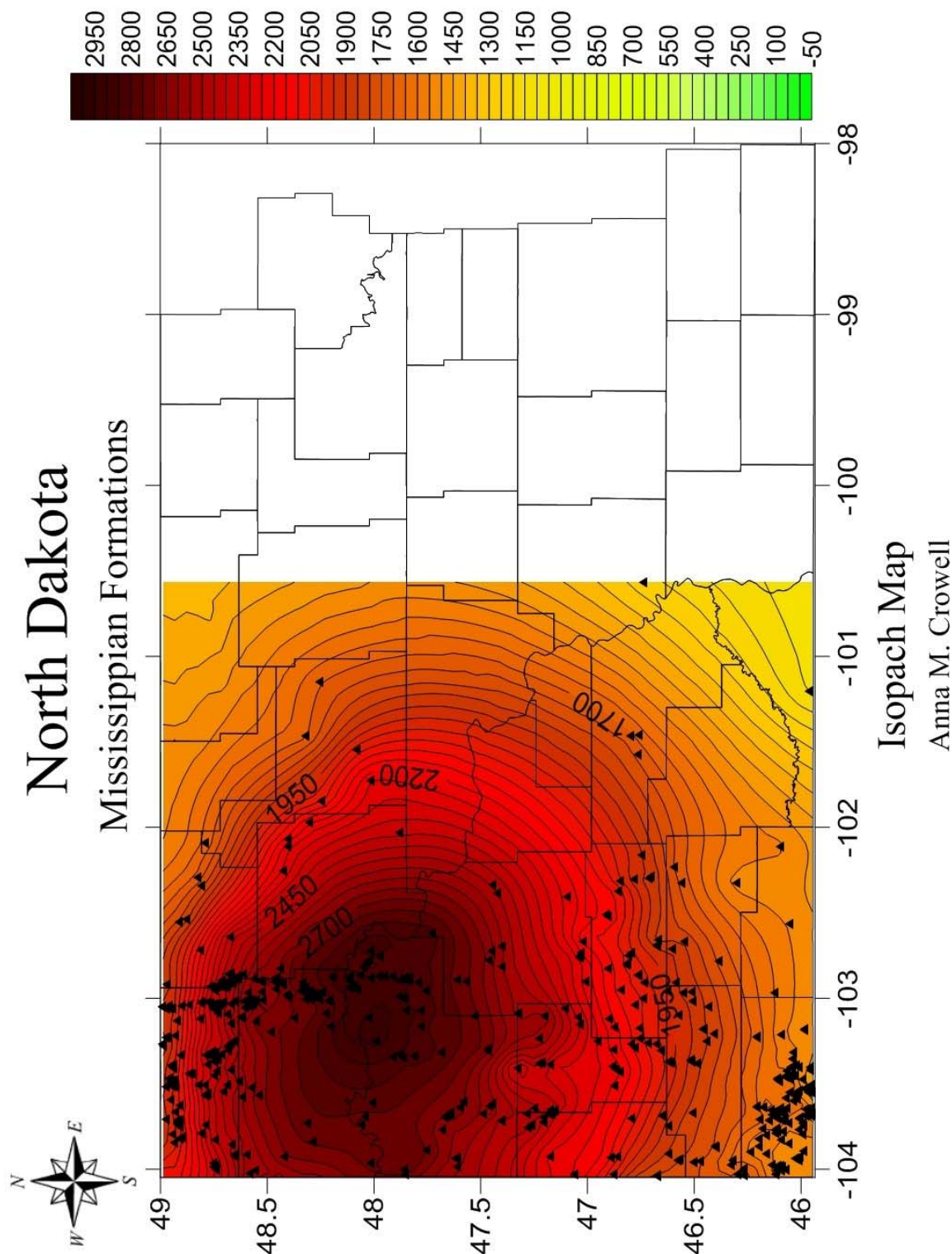


Figure 18 -- Isopach map of the Mississippian formations

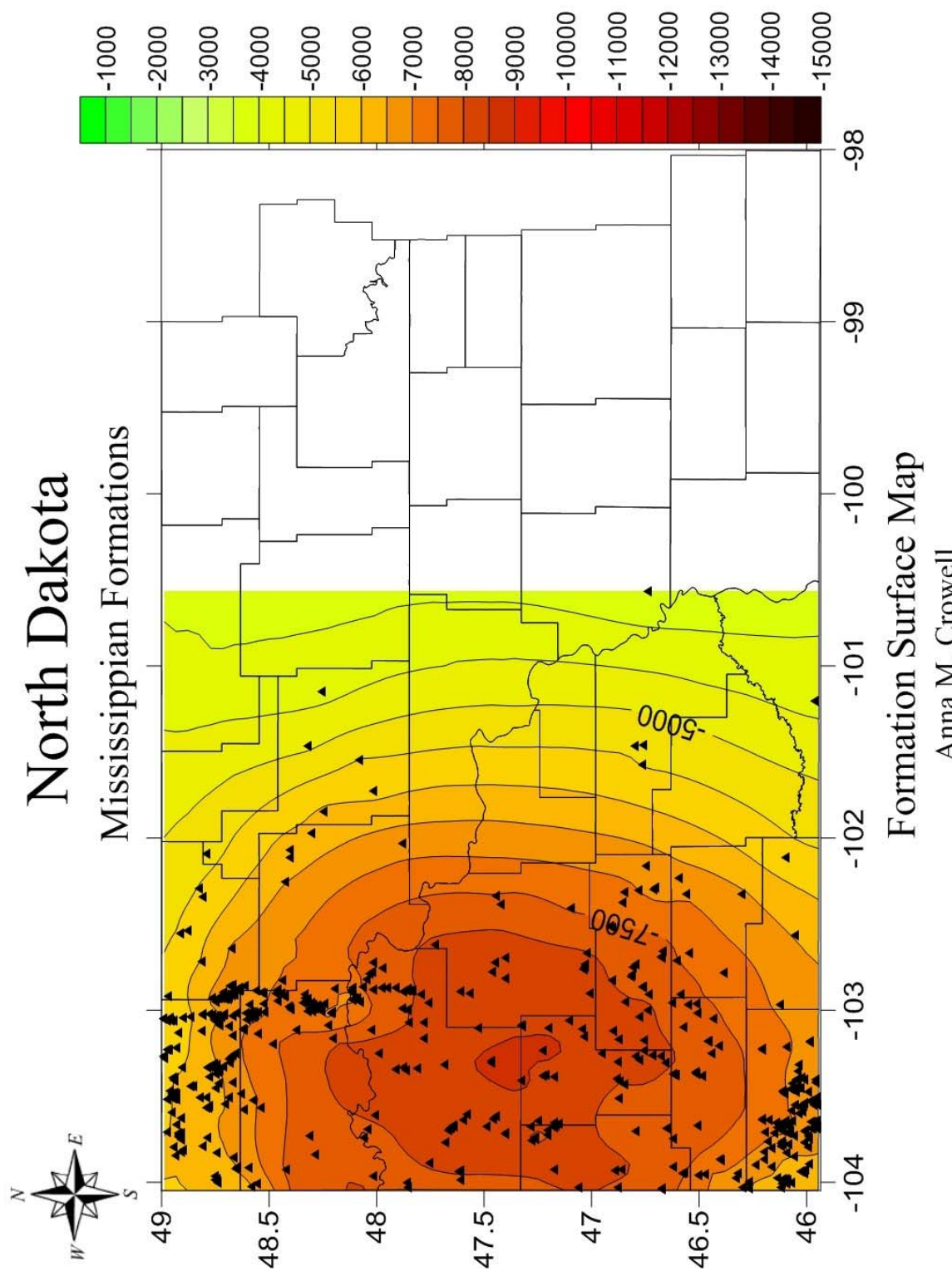


Figure 19 -- Formation surface map of the Mississippian formations

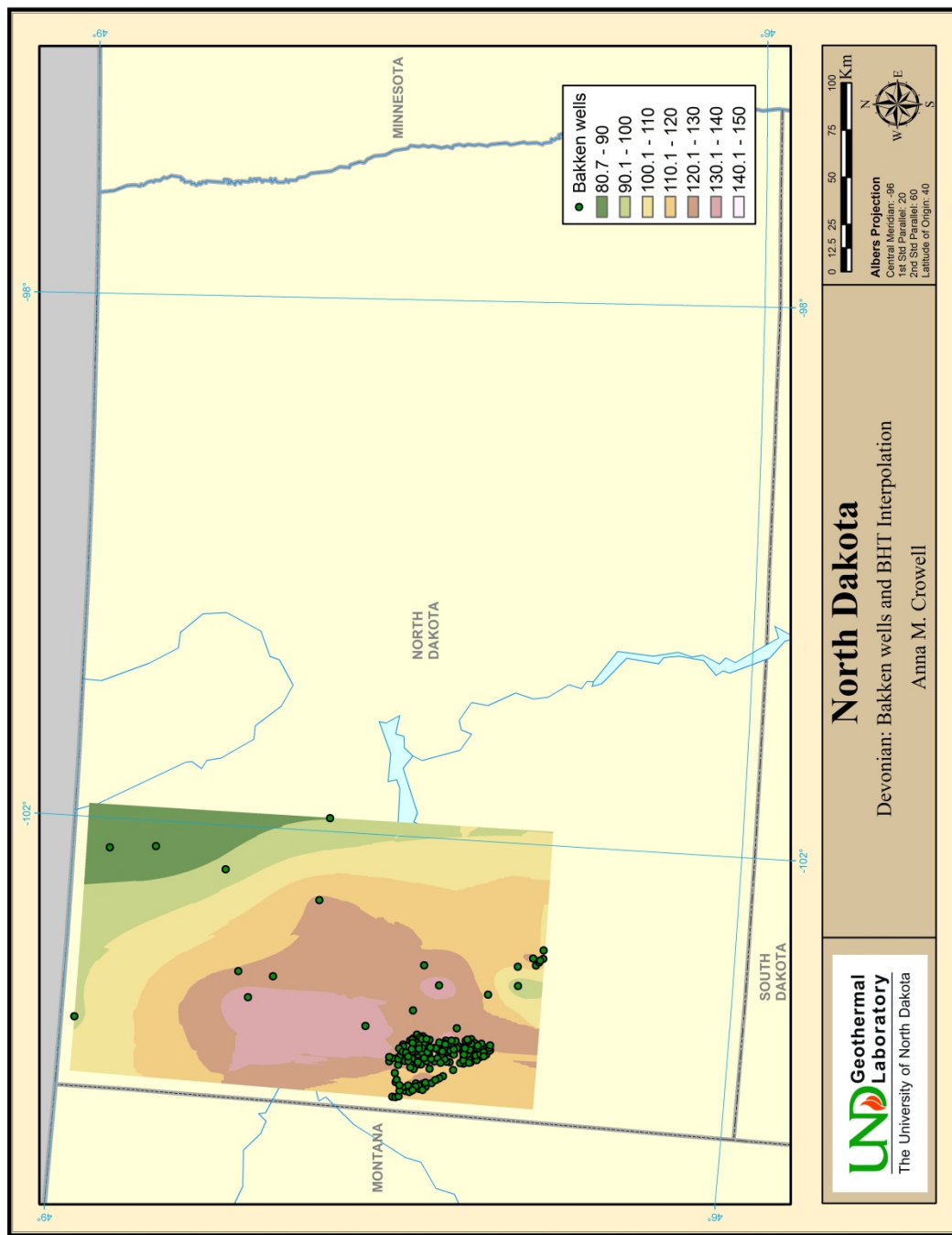


Figure 20 -- Estimate of the reservoir area of the Bakken formation

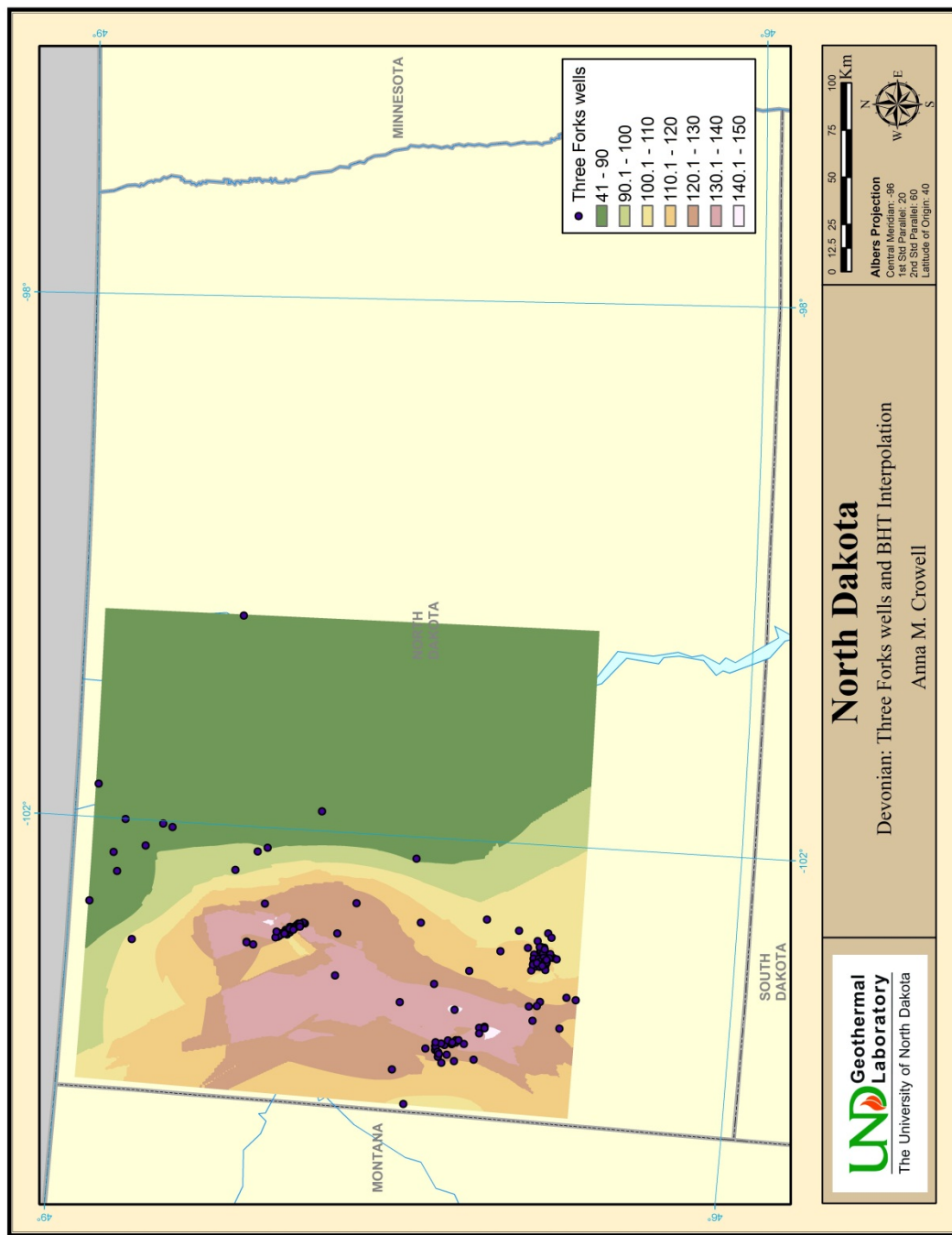


Figure 21 -- Estimated reservoir area of the Three Forks formation

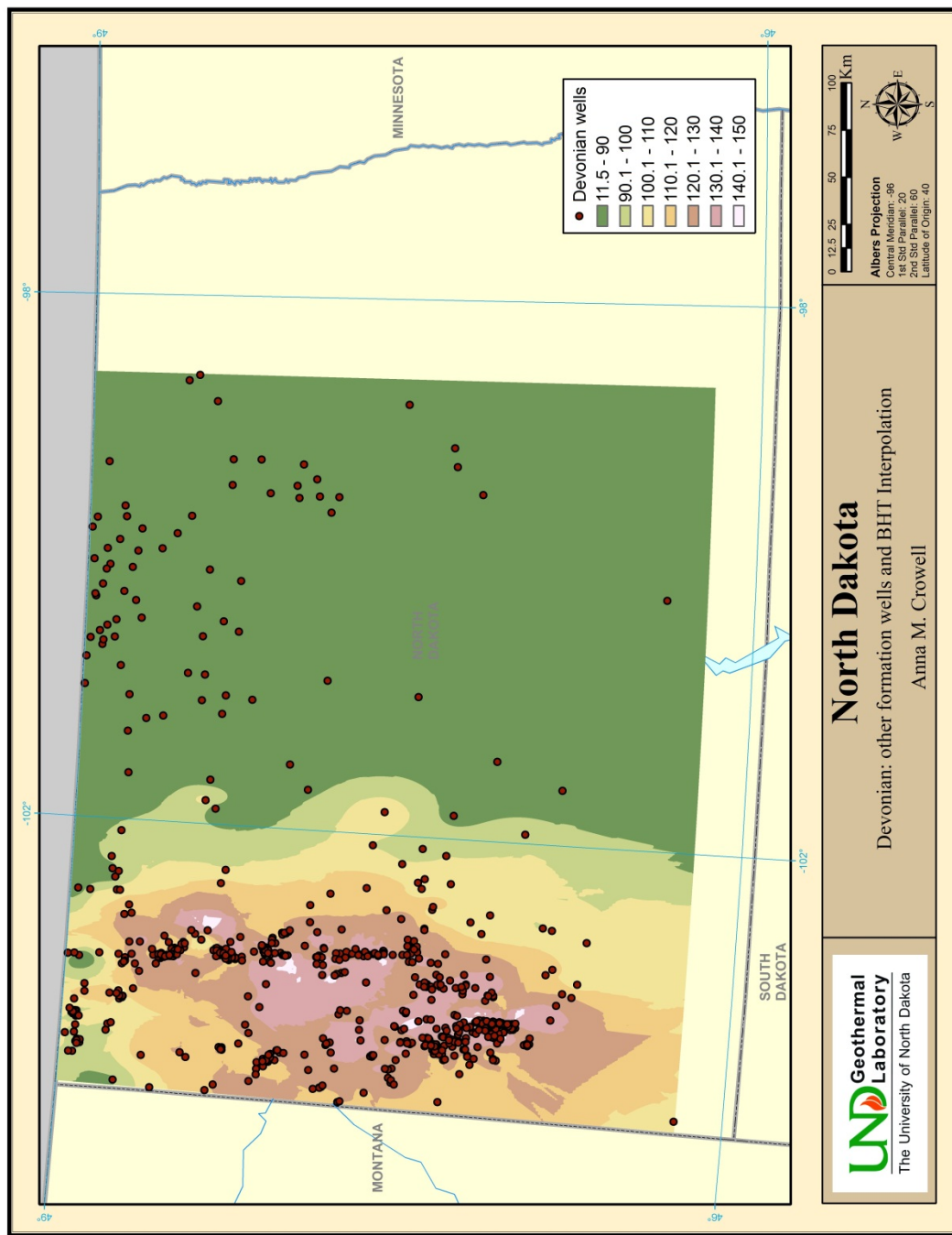


Figure 22 -- Estimate of the reservoir area for the other Devonian formations

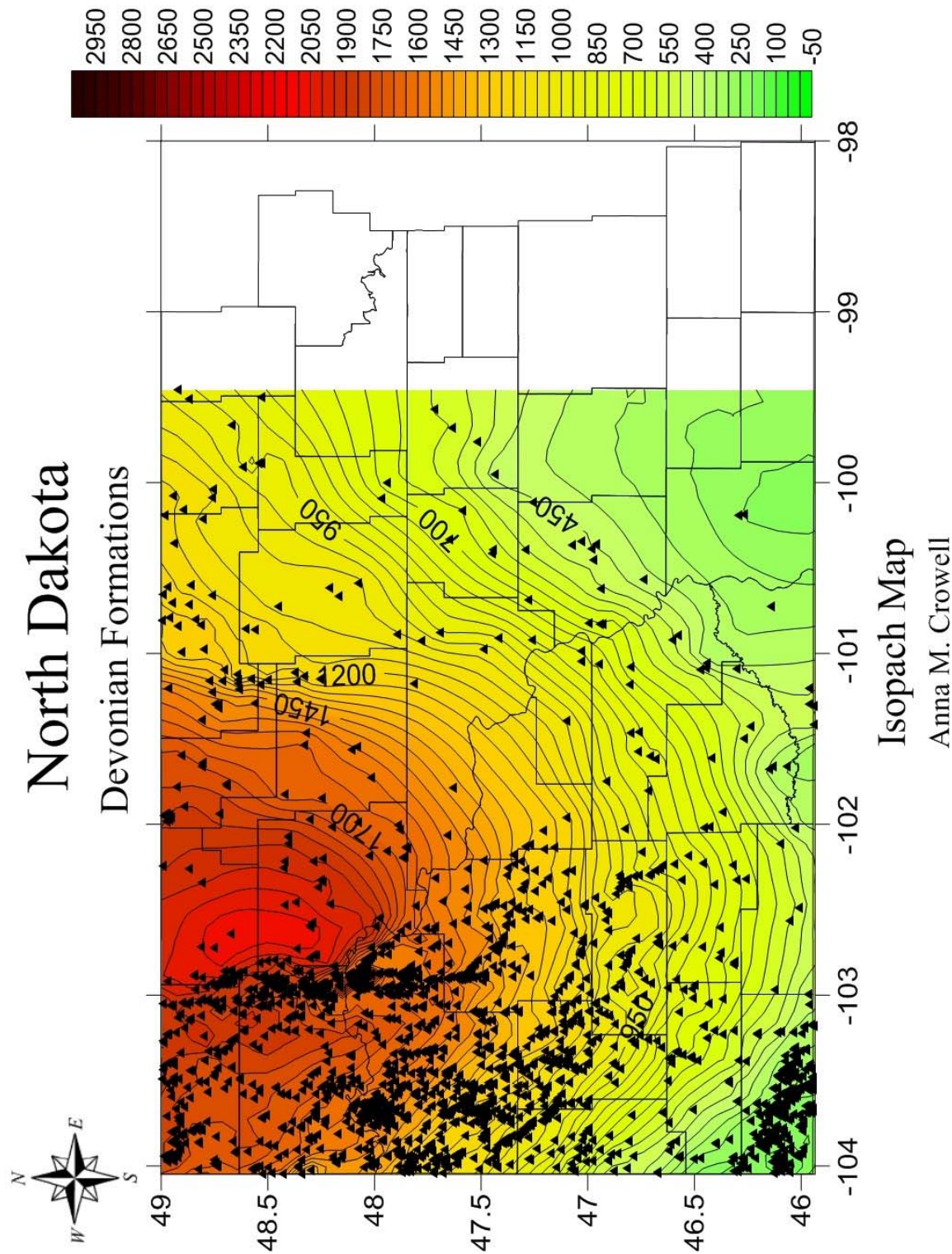


Figure 23 -- Isopach Map of Other Formations in the Devonian Period

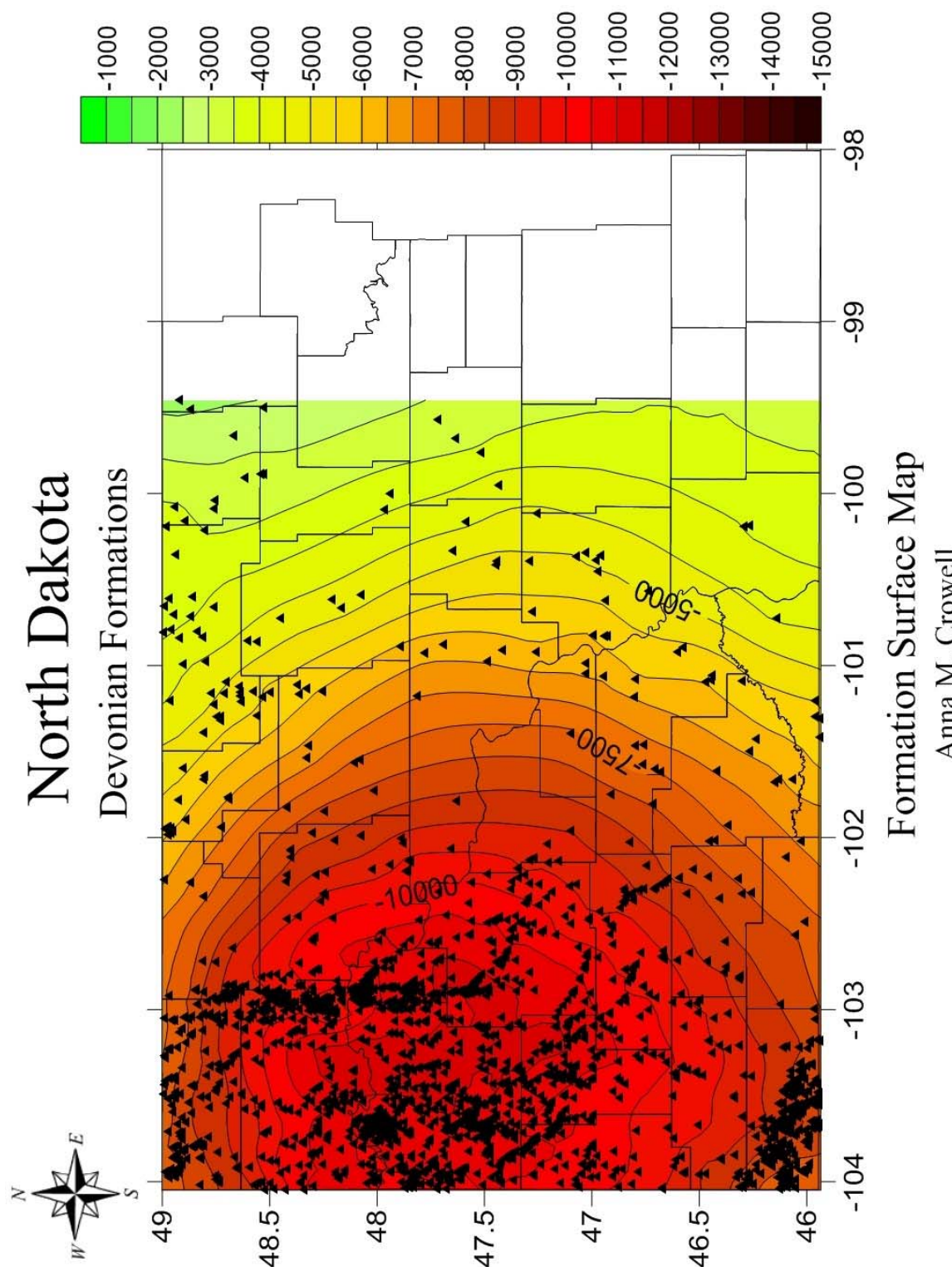


Figure 24 -- Formation surface map of the Devonian formations

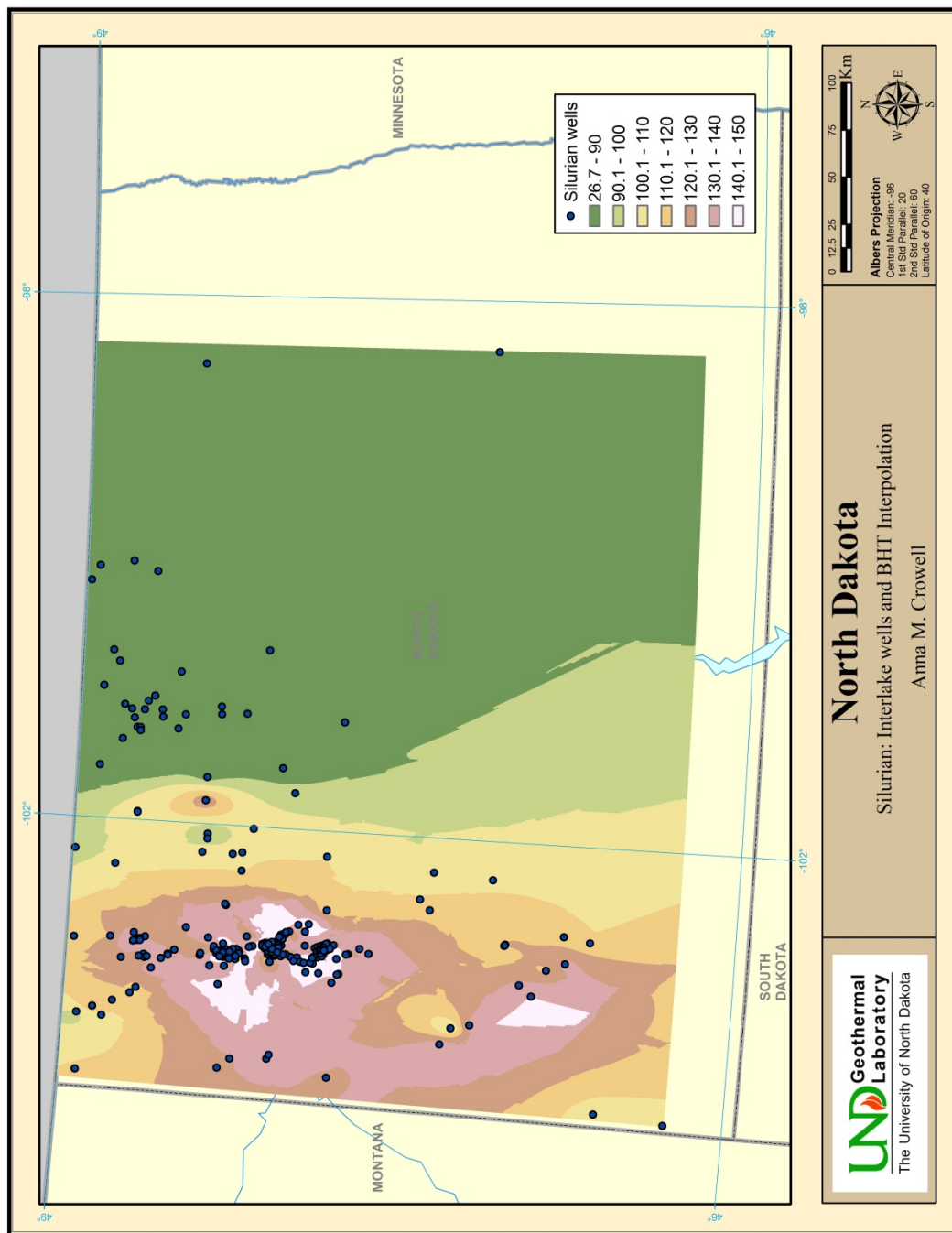


Figure 25 -- Estimate of the reservoir area for the Silurian Interlake formation

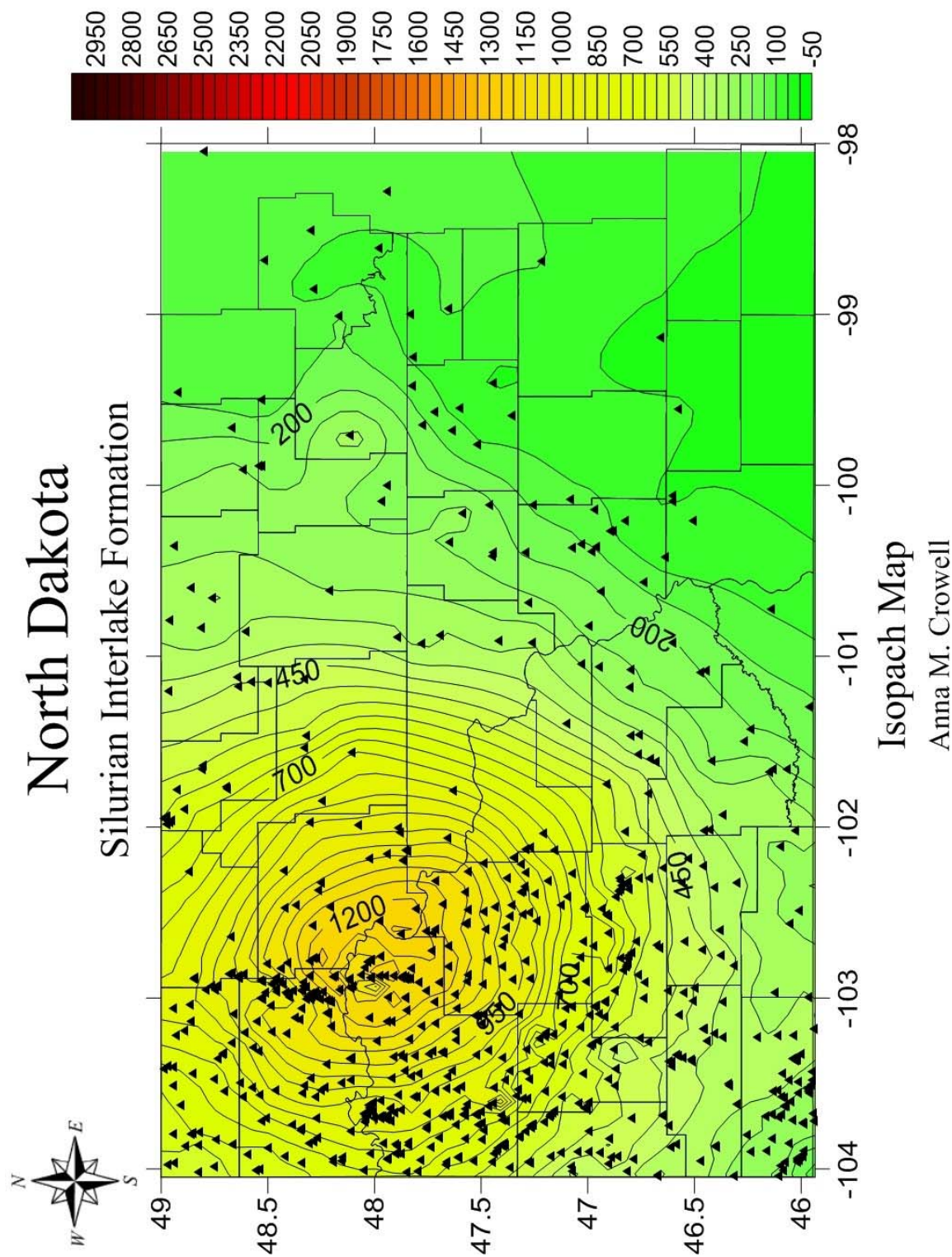


Figure 26 -- Isopach map of the Silurian Interlake formation

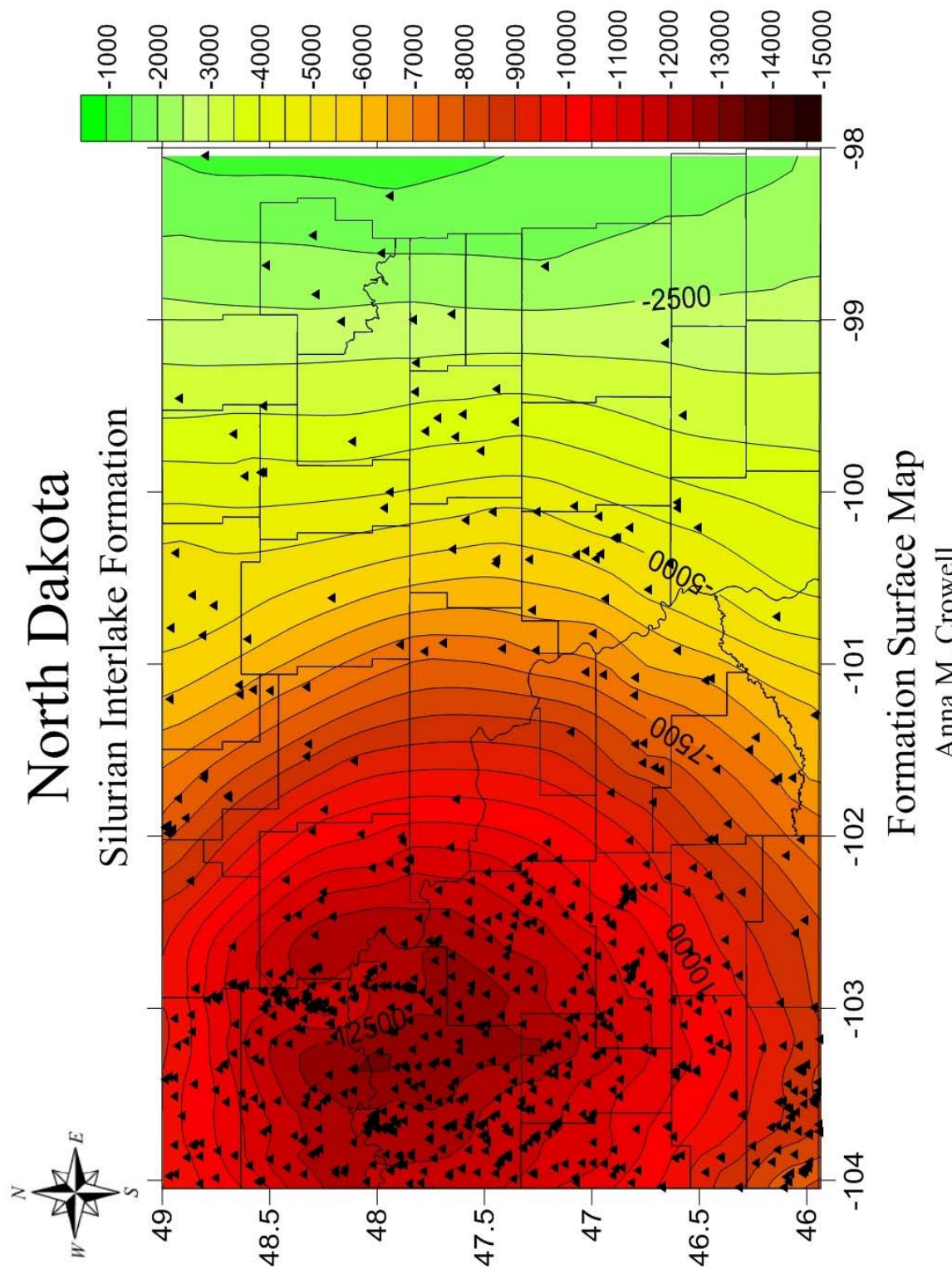


Figure 27 -- Formation surface map of the Silurian Interlake formation

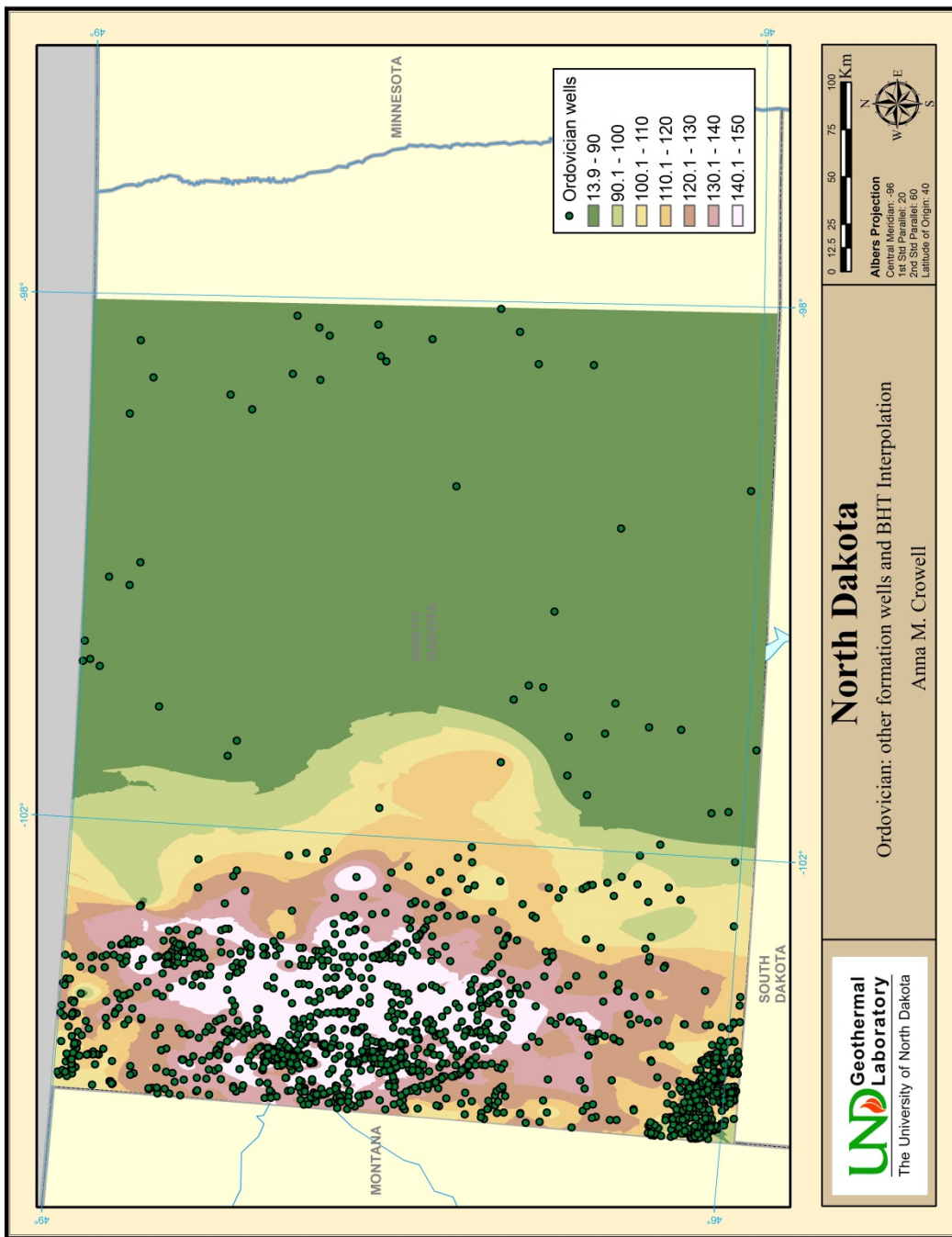


Figure 28 -- Estimate of the reservoir area for the other Ordovician formations

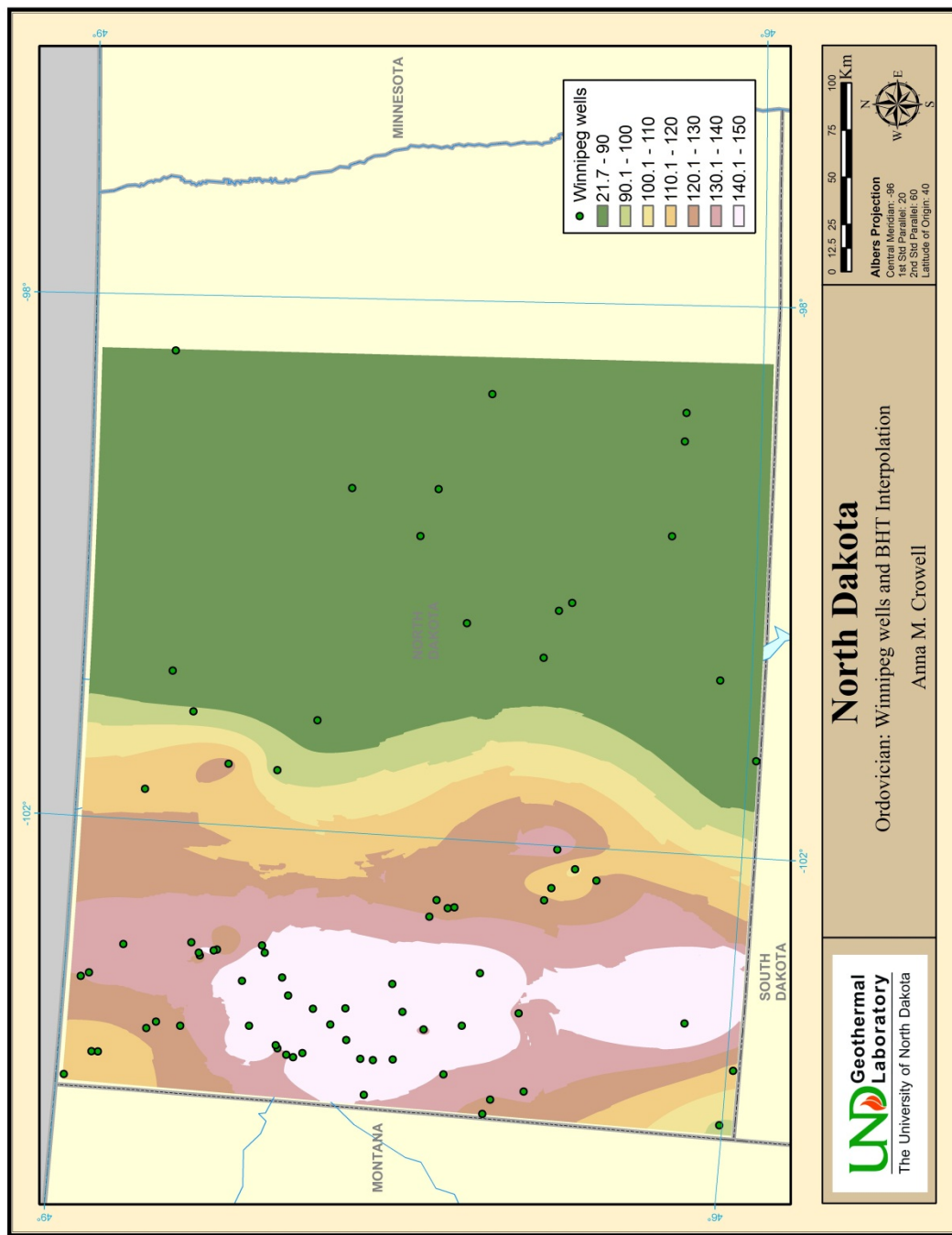


Figure 29 -- Estimate of the reservoir area for the Winnipeg formations

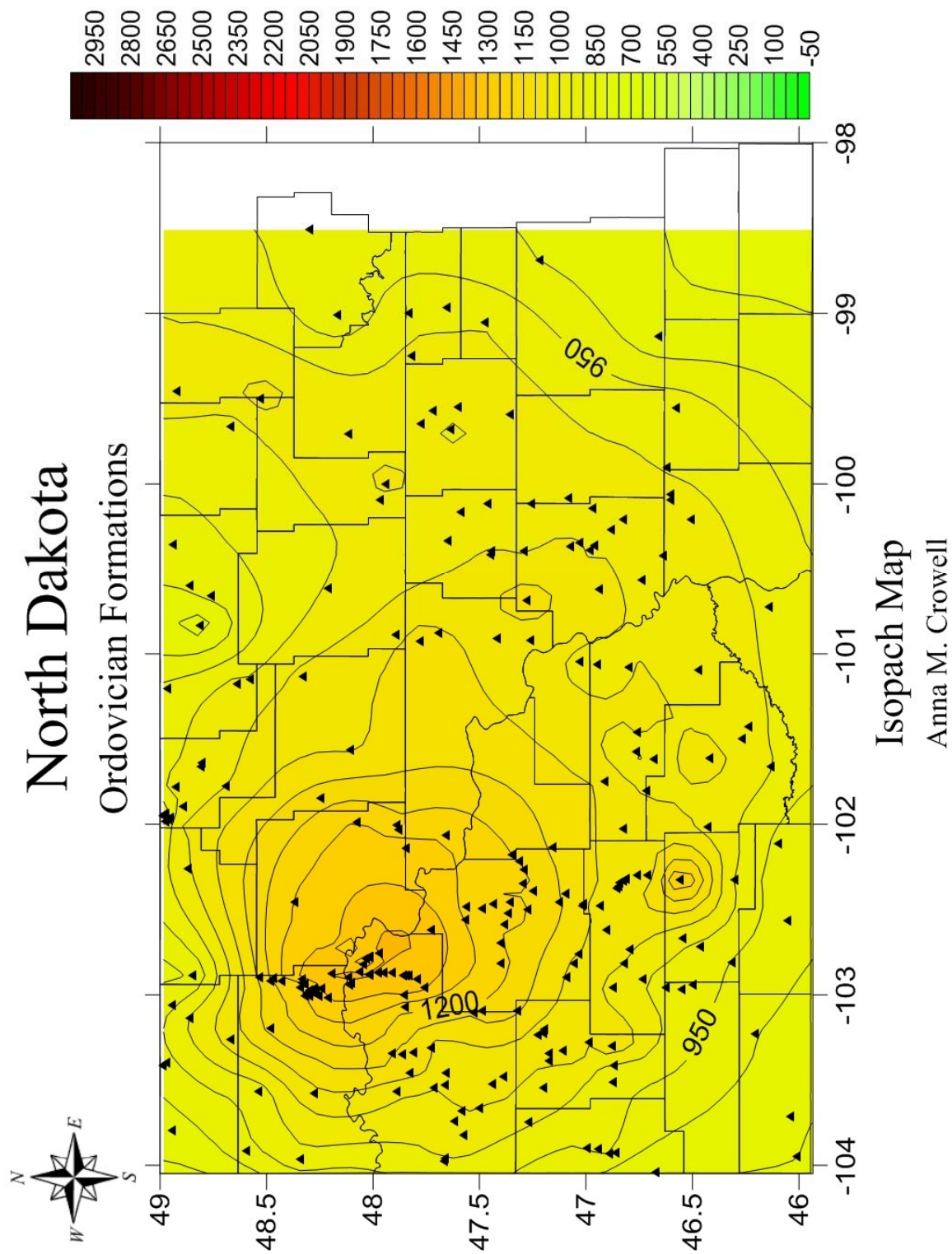


Figure 30 -- Isopach Map for the Ordovician formations

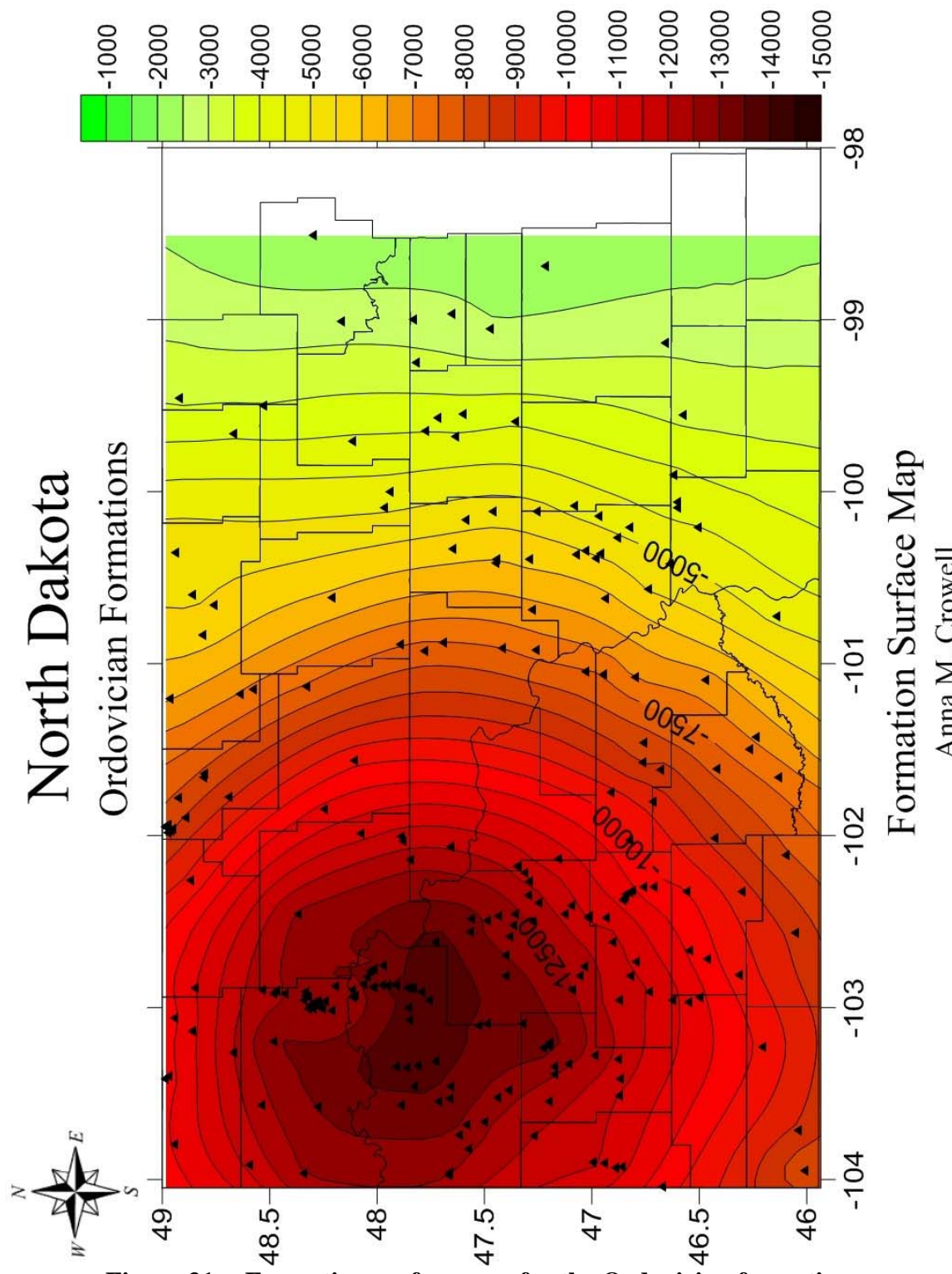


Figure 31 -- Formation surface map for the Ordovician formations

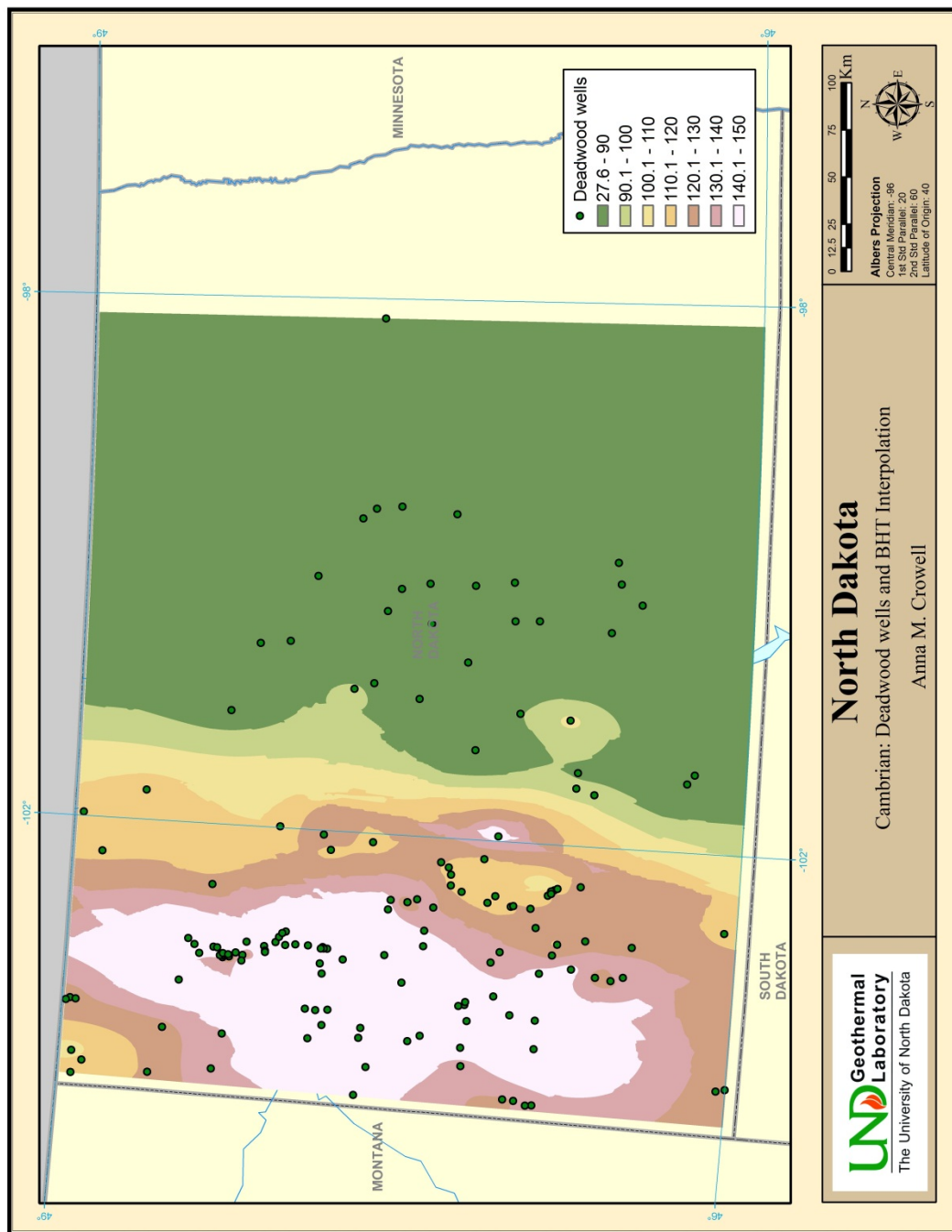


Figure 32 -- Estimate of the reservoir area for the Deadwood formation

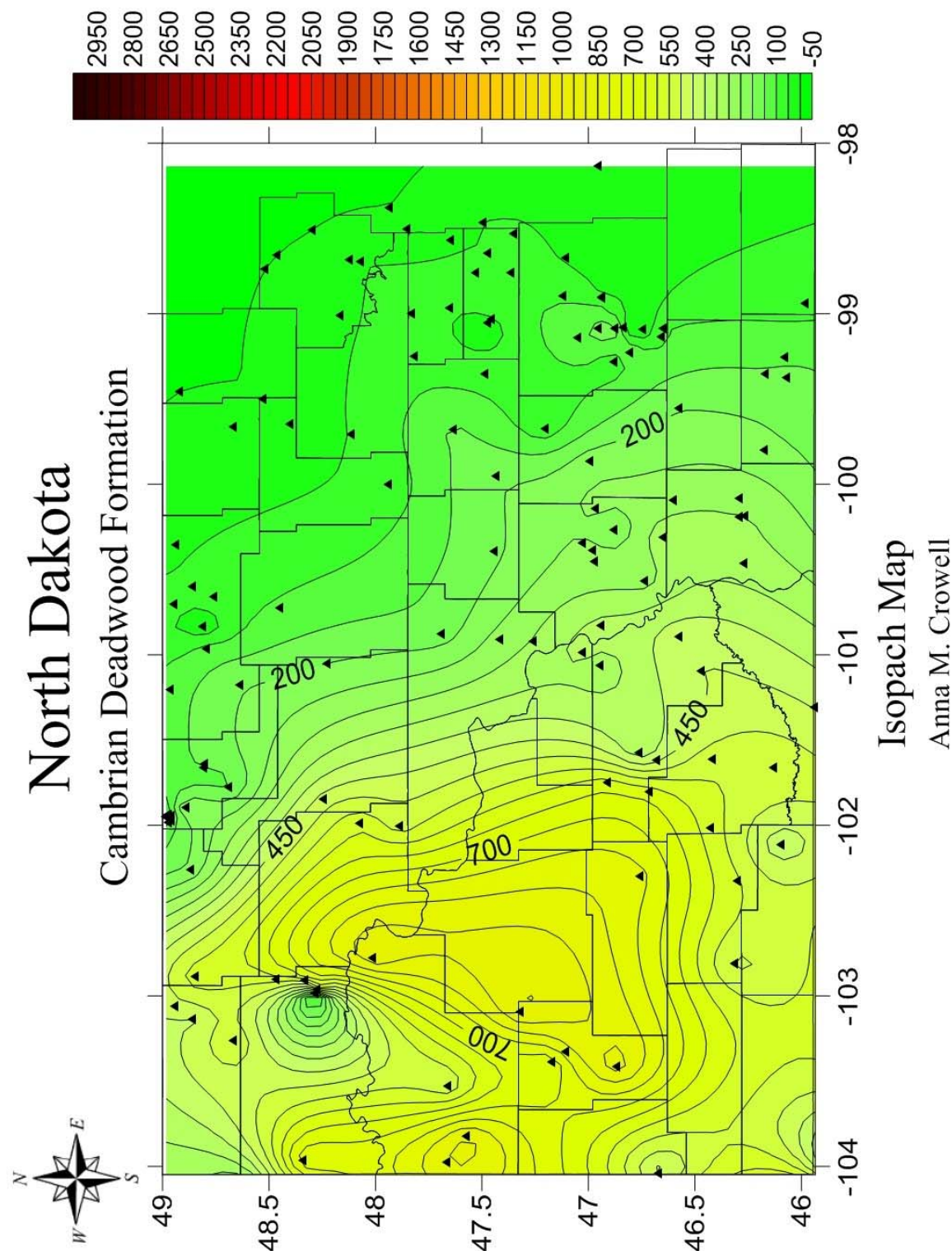


Figure 33 -- Isopach map of the Cambrian Deadwood formation

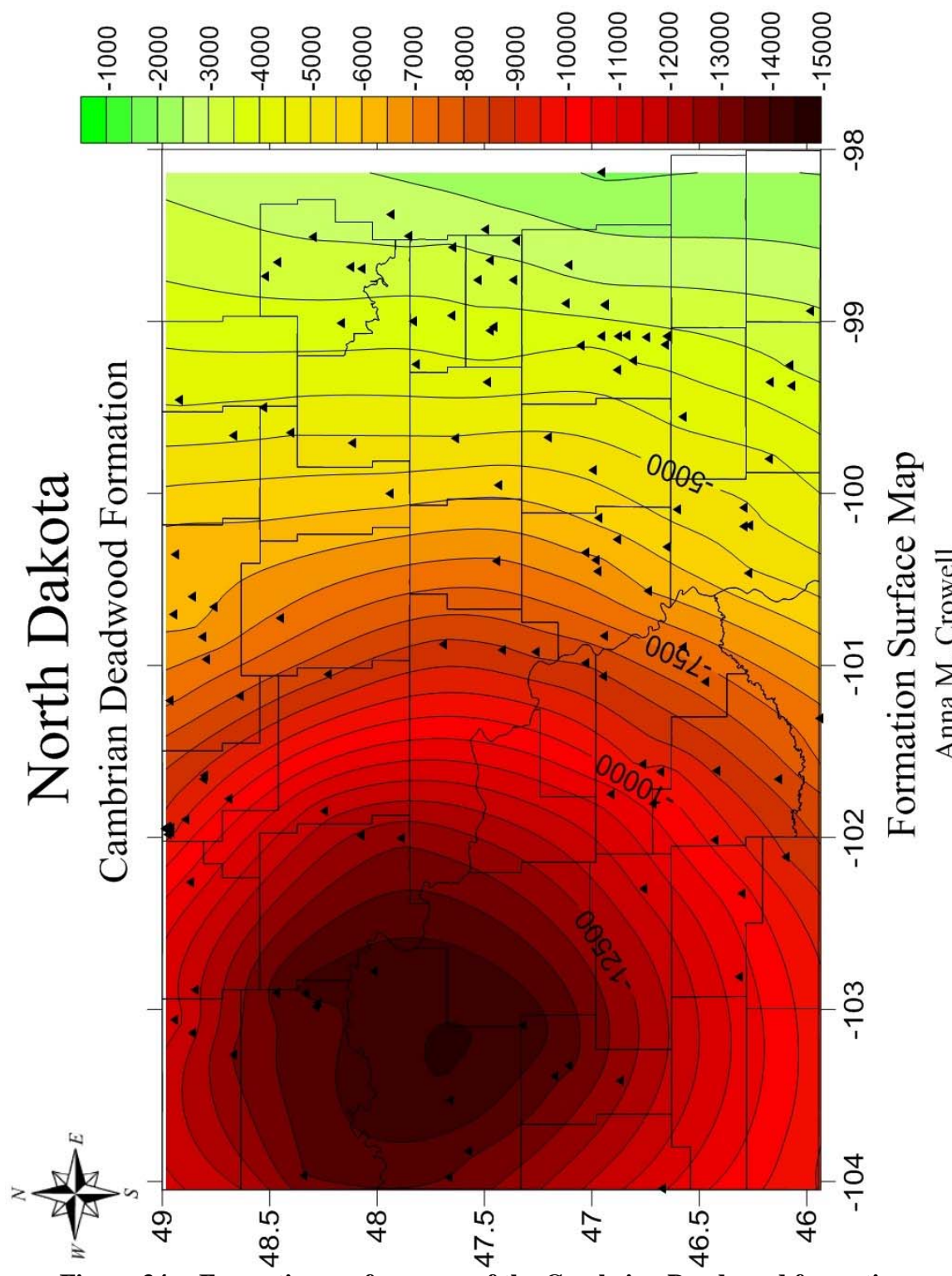


Figure 34 -- Formation surface map of the Cambrian Deadwood formation

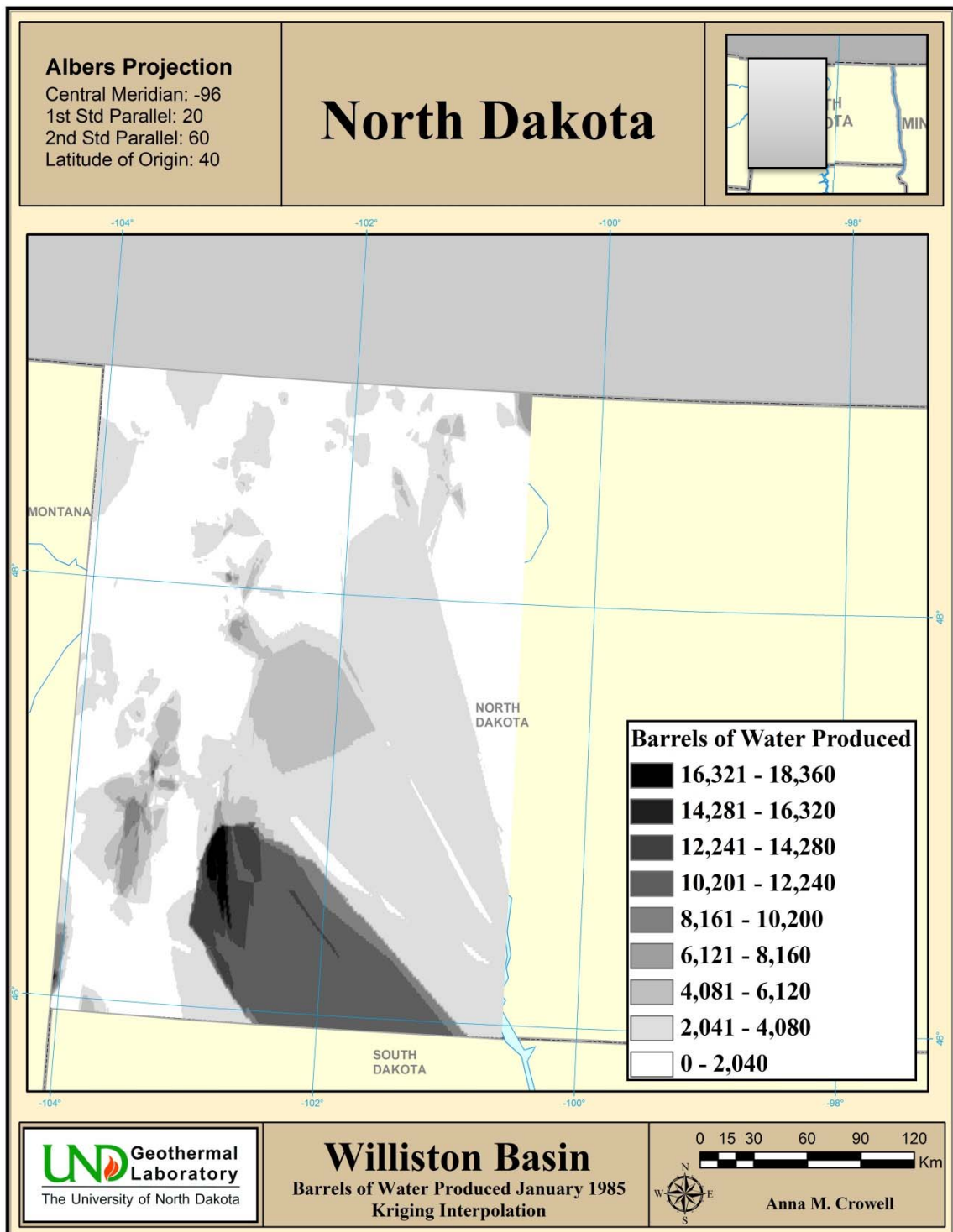


Figure 35 -- Raster image of the January 1985 BBL data interpolated

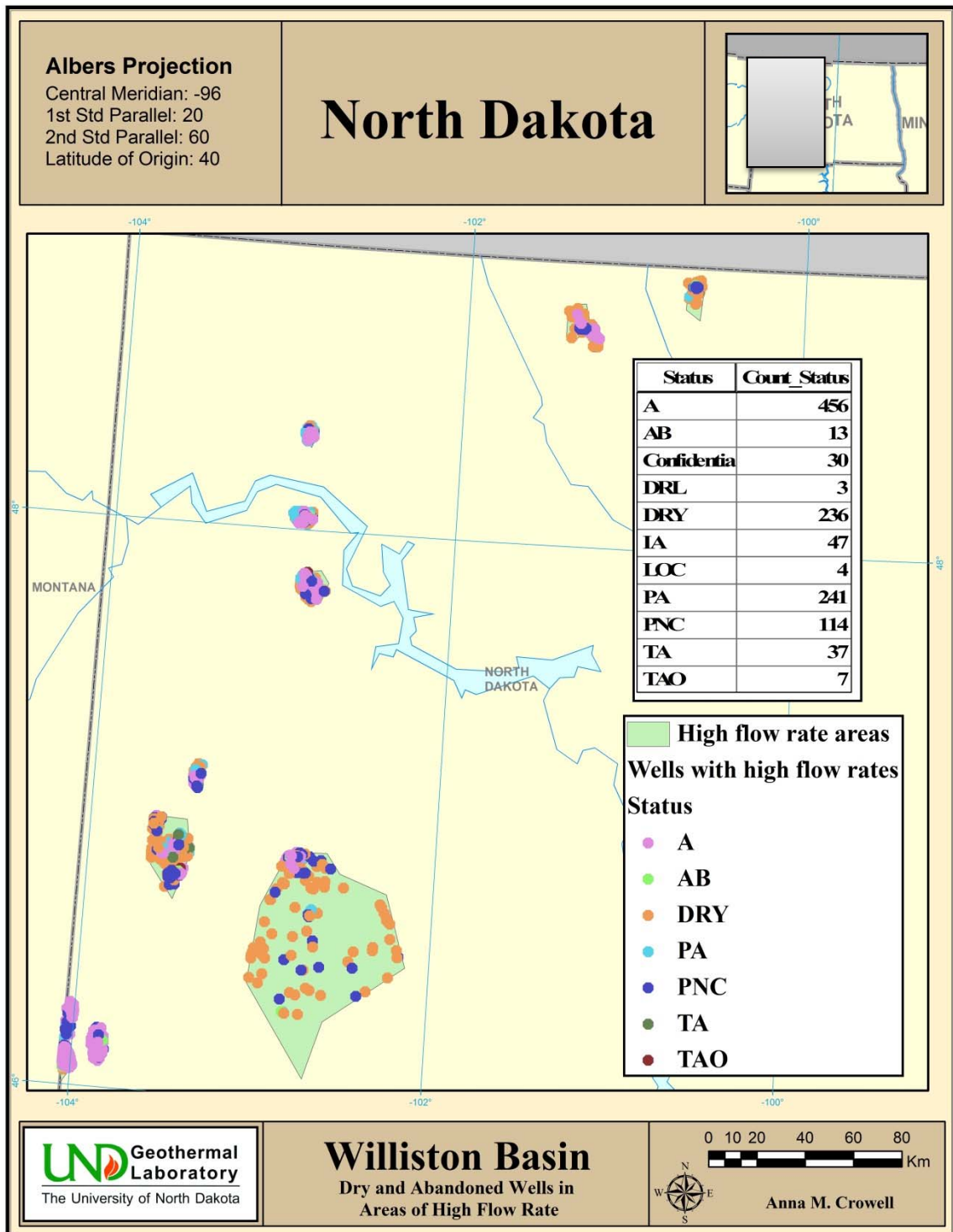


Figure 36 -- Abandoned and Dry Wells in High Flow Rate Areas

APPENDIX B

Tables

Form./Grp./Sys.	90°-100°C	100°-110°C	110°-120°C	120°-130°C	130°-140°C	140°-150°C	150°C +
Tyler	9.18×10^{15} J	1.15×10^{16} J	8.53×10^{15} J	--	--	--	--
Mississippian	2.06×10^{18} J	1.57×10^{18} J	3.06×10^{18} J	3.55×10^{18} J	1.85×10^{18} J	--	--
Devonian	1.74×10^{18} J	1.98×10^{18} J	1.48×10^{18} J	1.39×10^{18} J	8.91×10^{17} J	8.38×10^{17} J	8.75×10^{17} J
Silurian	1.07×10^{18} J	7.21×10^{17} J	4.44×10^{17} J	6.32×10^{17} J	4.04×10^{17} J	3.86×10^{17} J	1.05×10^{17} J
Ordovician	1.44×10^{18} J	1.36×10^{18} J	2.17×10^{18} J	2.07×10^{18} J	1.92×10^{18} J	1.27×10^{18} J	1.15×10^{18} J
Cambrian	5.59×10^{17} J	1.67×10^{17} J	4.12×10^{17} J	5.25×10^{17} J	4.22×10^{17} J	3.04×10^{17} J	2.34×10^{17} J

Table 1 – Energy for each Formation/Group/System listed by temperature range

Temp Range	90°-100°C	100°-110°C	110°-120°C	120°-130°C	130°-140°C	140°-150°C	150°C +
Rock Volume	65,167.9 km ³	51,673.1 km ³	48,174.2 km ³	44,626.1 km ³	26,213.4 km ³	11,696.9 km ³	8,825.8 km ³
Water Volume	4,037.2 km ³	3,091.9 km ³	2,891.5 km ³	2,723.3 km ³	1,594.7 km ³	726.3 km ³	530.2 km ³
Thermal Energy	6.88 x 10 ¹⁸ J	6.81 x 10 ¹⁸ J	7.57 x 10 ¹⁸ J	8.17 x 10 ¹⁸ J	5.49 x 10 ¹⁸ J	2.80 x 10 ¹⁸ J	2.36 x 10 ¹⁸ J
Power Availability	2.15 x 10 ⁹ MW	1.89 x 10 ⁹ MW	2.10 x 10 ⁹ MW	2.27 x 10 ⁹ MW	1.52 x 10 ⁹ MW	7.78 x 10 ⁸ MW	6.56 x 10 ⁸ MW

Table 2 – Volume and Energy totals for the Williston Basin

Temp Range (°C)	Total Energy (J)	Recoverable (J)	Efficiency			
			6.7% MWh	10% MWh	12% MWh	14% MWh
90-100	6.88×10^{21}	6.88×10^{18}	1.44×10^8	2.15×10^8	2.58×10^8	3.01×10^8
100-110	6.81×10^{21}	6.81×10^{18}	1.27×10^8	1.89×10^8	2.27×10^8	2.65×10^8
110-120	7.57×10^{21}	7.57×10^{18}	1.41×10^8	2.10×10^8	2.52×10^8	2.95×10^8
120-130	8.17×10^{21}	8.17×10^{18}	1.52×10^8	2.27×10^8	2.72×10^8	3.18×10^8
130-140	5.49×10^{21}	5.49×10^{18}	1.02×10^8	1.52×10^8	1.83×10^8	2.13×10^8
140-150	2.80×10^{21}	2.80×10^{18}	5.21×10^7	7.78×10^7	9.33×10^7	1.09×10^8
150 +	2.36×10^{20}	2.36×10^{18}	4.39×10^7	6.56×10^7	7.87×10^7	9.18×10^7

Table 3 - The estimated recoverable power based on the range of binary power plant efficiencies.

APPENDIX C

List of Acronyms

AAPG	American Association of Petroleum Geologists
API	American Petroleum Institute
BHT	Bottom-hole temperature
C	Celsius
GIS	Geographical Information System
GSNA	Geothermal Survey of North America
J	Joules
K	Kelvin
km	kilometer
kWe	killiwatts electric
L/s	Liters per second
m	Meters
Mt/yr	Megaton per year
MW	Megawatt
MWe	Megawatts electric
mW/m²	milliwatts per meter squared
NAD83	North America Datum, 1983
OCR	Optical Character Recognition
PSCWi	Public Service Commission of Wisconsin
SMU	Southern Methodist University
Tcf	Temperature correction factor
TD	Total Depth

SOURCES CITED

Birch, F., 1950, Flow of Heat in the Front Range, Colorado, Bulletin of the Geological Society of America, vol. 61, p. 567-630.

Blackwell, D.D., 1971, The Thermal Structure of the Continental Crust, *in* The Structure and Physical Properties of the Earth's Crust, Geophysical Monograph 14, ed. J.G. Heacock, p. 169-184.

Blackwell, D. D. and J. L. Steele, 1989, Thermal Conductivity of Sedimentary Rocks: Measurement and Significance, Thermal History of Sedimentary Basins: Methods and Case Histories, p. 13-36.

Blackwell, D. D., J. L. Steele, and L. C. Carter, 1991. Heat Flow Patterns of the North American Continent: A Discussion of the DNAG Geothermal Map of North America, Neotectonics of North America: Boulder, Colorado, Geological Society of America, Decade Map, vol. 1.

Blackwell, D.D., and M. Richards, 2004. Geothermal Map of North America, U.S. Subset. Amer. Assoc. Petroleum Geologists, Tulsa, OK, scale 1:6,500,000.

Blackwell, D. D., and Richards, M., 2004a, Calibration of the AAPG Geothermal Survey of North America BHT Data Base: American Association of Petroleum Geologists Annual Meeting 2004, Dallas, Texas, Poster session, paper 87616.

Carlson C.G., and S.B. Anderson, 1965, Sedimentary and Tectonic History of North Dakota Part of Williston Basin, Bulletin of the American Association of Petroleum Geologists, vol. 49, no. 11, p. 1833-1849.

Crough, S. T. and G. A. Thompson, 1976, Thermal Model of Continental Lithosphere, Journal of Geophysical Research, vol. 81, no. 26, p. 4857-4862.

Gosnold Jr., W. D., 1984, Geothermal Resources in the Williston Basin: North Dakota, Transactions of the Geothermal Resources Council, vol. 8, p. 431-436.

Gosnold, W. D., 1990, Heat flow in the Great Plains of the United States, Journal of Geophysical Research, vol. 95, no. B1, p. 353-374.

Gosnold, W.D., Jr., 1991, Subsurface Temperatures in the Northern Great Plains, *in* Slemmons, D.B., E.R. Engdahl, M.D. Zoback, and D.D. Blackwell, eds., Neotectonics of North America; Boulder, Colorado, Geological Society of America, Decade Map vol. 1.

Gosnold, W. D., P. E. Todhunter, and W. Schmidt, 1997, The Borehole Temperature Record of Climate Warming in the Mid-continent of North America, *Global and Planetary Change*, vol. 15, no. 1-2, p. 33-45.

Harrison W.E., K.V. Luza, M.L Prater, and P.K. Chueng, 1983, Geothermal resource assessment of Oklahoma, *Oklahoma Geological Survey, Special Publication 83-1*.

Heck T.J., R.D. LeFever, D.W. Fischer, and J. LeFever, Overview of the Petroleum Geology of the North Dakota Williston Basin, <<https://www.dmr.nd.gov/ndgs/Resources/WBPetroleumnew.asp>>, Accessed 12/30, 2010.

Herzog, H.J. and D. Golomb, 2004, Carbon Capture and Storage from Fossil Fuel Use, in C.J. Cleveland (ed.), *Encyclopedia of Energy*, Elsevier Science Inc., New York, p. 277-287.

Kehle, R. O., R. J. Schoepel, and R. K. Deford, 1970, The AAPG Geothermal Survey of North America, *Geothermics*, vol. 2, no. PART 1, p. 358-367.

Lachenbruch, A.H., 1970, Crustal Temperature and Heat Production: Implications of the Linear Heat-Flow Relation, *Journal of Geophysical Research*, vol. 75, no. 17, p. 3291-3300

Lachenbruch, A. H., and J. H. Sass, 1977, Heat flow in the United States and the Thermal Regime of the Crust, in *The Earth's Crust, Geophysics Monograph Series*, vol. 20, edited by J. G Heacock, pp. 626-675, AGU, Washington, D.C.

LeFever, Richard. Personal Communication, June 2010. Interviewer: Anna Crowell.

Lewis, T.J., and A.E. Beck, 1977, Analysis of Heat Flow Data – Detailed Observations in Many Holes in a Small Area, *Tectonophysics*, vol. 41, p. 41-59.

Lund, J. W., L. Bjelm, G. Bloomquist, and A. K. Mortensen, 2008, Characteristics, Development and Utilization of Geothermal Resources - A Nordic Perspective, *Episodes*, vol. 31, no. 1, p. 140-147.

Majorowicz, J. A., F. W. Jones, H. L. Lam, and A. M. Jessop, 1984, The Variability of Heat Flow Both Regional and with Depth in Southern Alberta, Canada: Effect of groundwater flow? *Tectonophysics*, vol. 106, no. 1-2, p. 1-29.

Majorowicz, J. A., F. W. Jones, and A. M. Jessop, 1986, Geothermics of the Williston Basin in Canada in Relation to Hydrodynamics and Hydrocarbon Occurrences. *Geophysics*, vol. 51, no. 3, p. 767-779.

McKenna, J. R. and D. D. Blackwell, 2005, Geothermal Electric Power from Hydrocarbon Fields, *Transactions of the Geothermal Resources Council*, vol. 29, p. 283-287.

Morgan, P., 1984, The Thermal Structure and Thermal Evolution of the Continental Lithosphere, *Physics and Chemistry of the Earth*, vol. 15, no. C, p. 107-193.

Morgan, P. and W.D. Gosnold, 1989, Heat Flow and Thermal Regimes in the Continental United States, *in* Pakiser, L.C., and W.D. Mooney, *Geophysical Framework of the continental United States*; Boulder, Colorado, Geological Society of America Memoir 172.

North Dakota Geological Survey, Oil and Gas Subscription Services;
<<https://www.dmr.nd.gov/oilgas/subscriptionservice.asp>> Accessed 12/30, 2010.

Pollack, H. N., 1982, The Heat Flow from the Continents. *Annual Review of Earth and Planetary Sciences*, vol. 10, p. 459-481.

Public Service Commission of Wisconsin, 2011, Electric Power Plants,
<http://psc.wi.gov/thelibrary/publications/electric/electric04.pdf>, Accessed 8/25/2011.

Roy, R. F., E. R. Decker, D. D. Blackwell, and F. Birch, 1968, Heat Flow in the United States, *Journal of Geophysical Research*, vol. 73, no. 16, p. 5207-5221.

Roy, R.F., D.D. Blackwell, and E.R. Decker, 1972, Continental Heat Flow, Chapter 19 *in* The Nature of the Solid Earth, ed. E.C. Robertson, p. 506-544, McGraw-Hill, New York.

Sanyal, S.K., L.E. Wells, and R.E. Bickham, 1979, Geothermal Well Log Interpretation: Midterm Report, Los Alamos Scientific Laboratory Informal Report LA-7693-MS.

Sass, J.H., A.H. Lachenbruch, R.J. Munroe, G.W. Greene, and T.H. Moses, Jr., 1971, Heat Flow in the Western United States, *Journal of Geophysical Research*, vol. 76, no. 26, p. 6376-6413.

Sclater, J. G., C. Jaupart, and D. Galson, 1980, The Heat Flow through Oceanic and Continental Crust and the Heat Loss of the Earth. *Reviews of Geophysics and Space Physics*, vol. 18, no. 1, p. 269-311.

Simmons, G., 1961, Anisotropic Thermal Conductivity, *Journal of Geophysical Research*, vol. 66, no. 7, p. 2269-2270.

Sloss L.L., 1963, Sequences in the Cratonic Interior of North America, *Geological Society of America Bulletin*, vol. 74, p. 93-93-114.

Sorey M.L. M. Nathenson, and C. Smith, 1982, Methods for Assessing Low-Temperature Geothermal Resources, *in* Reed, M.J., ed., *Assessment of Low-temperature Geothermal Resources of the United States -1982*: U.S. Geological Survey Circular 892, p. 17-29.

Steele, J.L., R.E. Spafford, and D.D. Blackwell, 1981, Collection, Reduction, and Analysis of Heat Flow and Geothermal Gradient Exploration Data, Transactions of the Geothermal Resources Council, vol. 5, p. 133-135.

Tester J.W., et. al., 2006. "MIT: The Future of Geothermal Energy. Impact of Enhanced Geothermal Systems [EGS] on the United States in the 21st Century." Massachusetts Institute of Technology.

Tüfekçi, N., M. Lütfi Süzen, and N. Güleç, 2009, GIS Based Geothermal Potential Assessment: A case study from Western Anatolia, Turkey, Energy, vol. 35, no. 1, p. 246-261.

U.S. Census Bureau. Current Population Reports: Projections of the Number of Households and Families in the United States: 1995 to 2010, P25-1129.

USGS, 1975. Assessment of Geothermal Resources of the United States - 1975. US Geological Survey Circular, no. 726.

USGS, 1978. Assessment of Geothermal Resources of the United States - 1978. US Geological Survey Circular, no. 790.

USGS, 1982. Assessment of Geothermal Resources of the United States - 1980. US Geological Survey Circular, no. 892.

Veil, J.A., M.G. Puder, D. Elcock, and R.J. Redweik, Jr, 2004, A White Paper Describing Produced Water from Production of Crude Oil, Natural Gas, and Coal Bed Methane, U.S. Department of Energy, National Energy Technical Laboratory, Contract No. W-31-109-Eng-38.

Williams, C.F., 2005, Evaluating Heat Flow as a Tool for Assessing Geothermal Resources, Proceedings, Thirtieth Workshop on Geothermal Reservoir Engineering, Stanford University, Stanford, California.

Yang Z., and C. Zu, 2010. "Methods of the Volume Measurement of Reservoir Using GIS: Research and Practice." Second International Conference on Technology, p. 237-240.